Theoretical Investigations of Structural Properties and Isomerization Mechanism of Weakly Bound Silicon Monocation Binary Carbonyl and Isocarbonyl Complexes

Yuxiang Bu,*,†,‡,§ Xinyu Song,† Xiangqian Hu,§ and Zhida Chen§

Institute of Theoretical Chemistry, Shandong University, Jinan 250100, P.R. China, Department of Chemistry, Qufu Normal University, Qufu 273165, P.R. China, and State Key Laboratory of Rare-Earth Materials Chemistry and Application, Peking University, Beijing 100871, P.R. China

Received: December 7, 2002; In Final Form: April 9, 2003

The structures, properties, and bonding character for the Si binary carbonyl and isocarbonyl monovalent cations, $Si(CO)_2^+$ ($^2B_1$), $COSiCO^+$ ($^2A''$), and $Si(OC)_2^+$ ($^2B_1$), in their doublet states have been investigated using four density functional theory (DFT) methods and the MP2 method with the 6-311+G* and aug-cc-pvtz basis sets. Results indicate that, for the binary carbonyl and isocarbonyl Si cations, there exist three stable isomers; all of them exhibit V-type structures in the doublet state, and no linear geometry has been found. The most stable isomer is $Si(CO)_2^+$ ($^2B_1$), the dicarbonyl Si cation, and can be assigned to the global energy minimum. The other two isomers are $COSiCO^+$ ($^2A''$), the carbonyl and isocarbonyl Si cation, and $Si(OC)_2^+$ ($^2B_1$), the di-isocarbonyl Si cation. They lie 22.8 and 40.9 kcal/mol above $Si(CO)_2^+$ ($^2B_1$) at the CCSD(T)/aug-cc-pvtz level. The calculated results and bonding analysis have indicated that the binding strength of CO with Si^+ by the C-terminal is stronger than that by the O-terminal, but the C−O bond weakening caused by the O-terminal interaction with Si^+ is slightly greater than that by the C-terminal. The corresponding coordination bond length to the Si^+ center by the O-terminal is significantly larger than that by the C-terminal. The vibrational frequencies and the charge populations also support the above analysis. These binary carbonyl or isocarbonyl Si complex cations have essentially silene cation character and should be referred to as binary carbonyl silene. Further comparison of the CO-binding energies among three binary carbonyl Si complex cations indicates that the second CO-binding energy (26.2 kcal/mol) of $Si(CO)_2^+$ ($^2B_1$) is greater by ∼5 kcal/mol than the first one (21.5 kcal/mol) at the CCSD(T,full)/6-311+G*//MP2(full)/6-311+G* level, but it is the inverse in the $Si(OC)_2^+$ ($^2B_1$) species. This observation, together with the bonding analysis, has implied that the possibility is small for the existence of the polycarbonyl Si cations with more than three CO's. To explore the state−state correlations among three isomers, searches of the transition states and the isomerization mechanism have also been performed. Results indicate that there are two single-ring transition states, which correlate with $Si(CO)_2^+$ ($^2B_1$) and $(CO)Si(CO)^+$ ($^2A''$) (TS1), and $(CO)Si(CO)^+$ ($^2A''$) and $Si(OC)_2^+$ ($^2B_1$) (TS2), respectively. The forward (inverse) activation energies are 29.6 kcal/mol (12.0 kcal/mol) for TS1 and 20.0 kcal/mol (6.9 kcal/mol) for TS2, respectively. No direct correlation is found for $Si(CO)_2^+$ ($^2B_1$) and $Si(OC)_2^+$ ($^2B_1$). The isomerizations for this kind of weak interaction system generally adopt the loosening−rotating mechanism.

1. Introduction

In view of the important interest in the biological and materials area, the interaction between carbon monoxide (CO) and nontransition metals and nonmetals has been the subject of many studies over recent years. A series of new progresses concerning the binding of CO have indicated that CO may be also significantly bonded to nontransition metal and nonmetal clusters, compounds, and nucleophilic and electrophilic centers-containing molecules, because of its strong ability of donating and accepting electrons. Therefore, the detailed investigations regarding the interaction between CO and various clusters and compounds are very interesting for the approaches to the functionality and its control mechanism of the biological and materials molecules. However, although great progresses have been made for these kinds of systems, studies on the interaction between CO and the nontransition metals or the nonmetals have appeared to be seriously absent. To our knowledge, only a few theoretical and experimental studies on such a kind of system have been reported. These works have mainly focused on the alkali carbonyls, $(M^+(CO)_n)$, $M(CO)_n$, $n = 1, 2, 3$ and M = H, Li, Na, K.[1−5] The emphasized properties are only on the bond dissociation energies of X^+-CO (X = H, Li, Na, and K),[2] the lithium and sodium action affinities of CO,[3] and the sequential bond energies of $M^+(CO)_n$ ($n = 1$ or 2 or 3; M = Li, Na, K).[4] Especially in recent years, some increasing attentions have also been paid on the investigations regarding the interactions of CO with alkali metals and the nontransition metals.[5−20] The electronic structures and relevant properties have been investigated in detail using different theoretical methods for Li carbonyls (Li_2-CO,[5] LiC_2O_2,[6] $Li(CO)_n$ ($n = 1, 2, 3$)[7]), Na and K carbonyls, Al carbonyls (AlCO, $Al(CO)_2$),[8−11] Al isocarbonyls (AlOC) and the AlCO cyclic structure,[9,11] and so forth. However, the studies on the nonmetal carbonyls have been found to be much more scarce than those on the nontransition metal carbonyls. Only a part of the subcarbonyl complexes have been experimentally detected by different groups for $AsCO^-$, AsCO,[12]

* To whom correspondence should be addressed at Shandong University.
† Shandong University.
‡ Qufu Normal University.
§ Peking University.

10.1021/jp027651x CCC: $25.00 © 2003 American Chemical Society
Published on Web 06/28/2003

$SiCO^-$, $GeCO^-$,[13] BCO, $(BCO)_2$, $B(CO)_2$,[14] SCO,[15,16] CCO,[17,18] and $Si(CO)_n$ ($n = 1, 2$),[19,20] but no detailed theoretical reports have been given on the studies of their various properties.

Due to the lack of the bonding active d orbitals, these nonmetal atoms will exhibit different bonding character from that of the transition metal atoms.

It is well-known that Si and Ge are important elements of semiconductor and noncrystalline materials; many works have focused on the Si-containing hydrocarbon-like compounds, and great progress has been made. Investigations indicate that silicon has a very different role in forming the hydrocarbon-like Si compounds from that of carbon in forming hydrocarbon compounds. After an experimental evidence was found that Si can bind one or two carbonyls to form SiCO and $Si(CO)_2$ under the cryogenic conditions,[19] Stolvik further determined experimentally the SiCO molecular geometry.[20] More recently, Scheafer's group has in detail explored the structures and properties for the Si mono-carbonyl complexes,[21−24] using couplet-cluster with single and double excitations (CCSD), configuration interaction with single and double excitations (CISD), and many triple-ζ basis sets. They investigated systematically the electronic structural characterization of silaketenylidene SiCO (carbonylsilene)[24] and 2-silaketenylidene CSiO[21] for their $^3\Sigma^-$ and $^3\Pi$ states, and they indicated that there is obviously a Renner−Teller effect only for the linear $^3\Pi$ state. They also reassigned the structure of dicarbonyl Si ($Si(CO)_2$ $^1A_1$) on the basis of theoretically predicted infrared spectra.[23] Obviously, these studies have provided much valuable information for the further investigation regarding the nonmetal carbonyls. However, these recent works have focused on only two low-lying triplet states ($^3\Sigma^-$, $^3\Pi$) for the monocarbonyl silicon and the low-lying singlet states ($^1\Sigma_g^+$, $^1A_1$) for the dicarbonyl Si, but no studies have been given for the binary carbonyl Si complex cation, $Si(CO)_2^+$, and its isomers.

The aim of this work is to give a detailed theoretical investigation on the geometrical parameters, the harmonic frequencies, the dissociation energies, the ionization potentials, and other relevant properties for $Si(CO)_2^+$, $COSiCO^+$, and $Si(OC)_2^+$ species at the doublet state, and to analyze the interconverting mechanism, using density functional theory methods and the wave function-correlated ab initio method with a relatively large one-particle basis set. Fortunately, in recent years the density functional theory (DFT) has emerged to be a reliable and computationally inexpensive method capable of successfully predicting the properties for many systems.[25−33] In particular, we have recently used these theoretical methods to investigate the structures and properties of the analogues (SiCO, $Si(CO)_2$) for which the relevant experimental data are available. The calculated character frequency for the C−O stretching vibration is within 1955−1984 cm^{-1} at several DFT levels,[32,33] being very close to the experimental value (1899 cm^{-1}).[19] These results also agree well with those at the other electron correlation levels, such as the CCSD method.[23,24] Similarly, there is good agreement between our calculated values and the other theoretical values. Thus, these DFT methods can be desirable to be applied to the calculations on these systems. The main objective is to accurately predict the geometries and the relevant quantities, to give reliable estimates of those fundamentals which are either masked or too weak to be observed in the matrix experiments, and to approach the isomerization mechanism for all possible isomers. This work may be predicted to provide some valuable information for the further investigations on the absorption interaction of carbonyl on the silicon-containing charged surface.

2. Calculational Details

The optimizations are first carried out for three silicon carbonyl isomers ($Si(CO)_2^+$, $COSiCO^+$, and $Si(OC)_2^+$) using the 6-311+G* basis set and the density functional theory (DFT) and the wave function-correlated Møller−Plesset perturbation theory. The four density functionals used are B3LYP, B3P86, B3PW91, and BHLYP, as implemented in Gaussian 98.[34] The former three models combine the Becke three-parameter hybrid functional, which is a linear combination of Hartree−Fock exchange, Slater exchange, and B88 gradient-corrected exchange,[35] with the correlation functionals of Lee, Yang, and Parr (LYP),[36,37] Perdew (P86),[38,39] and Perdew and Wang (PW91),[40] respectively, while the last one (BHLYP) is also a combination of half Hartree−Fock exchange, half LSDA, and half B88 gradient-corrected exchange with LYP correlational functionals. The used ab initio method is the second-order Møller−Plesset perturbation theory (MP2) with correlation correction by the valence and all electrons, respectively.

The geometries are first optimized using the DFT models described above. The harmonic vibrational frequencies are then obtained from analytic second derivative methods. Using the valence electron correlation MP2(fc) and the full electron correlation MP2(full) methods, the geometries are reoptimized, and the harmonic vibrational frequencies are calculated via finite differences of analytic gradients. All these optimizations and frequency calculations are at the 6-311+G* basis set level. The corresponding energy quantities are also calculated using the third-order and the fourth-order Møller−Plesset theories (MP3, MP4) with all substitutions, the coupled cluster singles and doubles including a perturbational estimate of the triples [CCSD(T)] with valence-electron or full-electron correlations. To establish the correlation among the found isomers, the transition state searches are then also carried out at the same theoretical levels. All isomers are correlated by the intrinsic reaction coordinate analysis. The calculations are performed with the Gaussian 98 program package. The calculations are mainly limited to the doublet state of these isomers for the bonding and charge distribution analysis and the determination of the ground state. The dissociation energies (D_e's) and the vertical electron affinities are then obtained by comparing the corresponding energy differences.

It should also be noted that at the present time the DFT has emerged as a reliable and computationally inexpensive method being capable of successfully predicting the properties of the difficult systems. It has been demonstrated that these methods can accurately predict the molecular properties of the systems that exhibit multireference character. Since DFT is computationally cheaper than post-Hartree−Fock methods, and its reliability has been demonstrated for difficult systems,[25−33] it is desirable to employ it for the calculations on these weak interaction systems.

Since the accuracy of DFT calculations also depends on the number of points used in the numerical integration, the more fine grids should be employed. However, for the comparison based on the energy difference, it is very important to use the same integration point numbers for all calculations. Thus, in all DFT calculations performed here, the numerical integrations of the functionals are carried out using a Gaussian 98 default grid consisting of 75 radial shells and 302 angular points per shell, resulting in about 7000 points per atom.

3. Results and Discussion

The geometry optimizations and the vibrational frequency calculations are first performed for ($Si^+ + 2CO$) systems at the

TABLE 1: Optimized Geometrical Parameters (Bond Length, Å; Bond Angle, deg) for Three Different Isomers $Si(CO)_2^+$, $Si(OC)_2^+$, and $COSiCO^+$ Using Different Methods with a 6-311+G* Basis Set

species	method	Si−C	C−O	∠SiCO	∠CSiC			
$Si(CO)_2^+$	B3LYP	1.9579	1.1247	167.0	82.2			
$^2B_1$	B3P86	1.9341	1.1238	167.2	81.4			
(A)	BHLYP	1.9765	1.1081	168.4	81.9			
	B3PW91	1.9389	1.1242	167.2	81.7			
	MP2(fc)	1.9762	1.1346	167.4	81.7			
	MP2(full)	1.9726	1.1338	167.5	81.6			
species	method	Si−C	C−O	∠SiCO	∠CSiO	Si−O	C−O	∠SiOC
$COSiCO^+$	B3LYP	2.0003	1.1261	174.2	80.4	2.3204	1.1429	165.2
($^2A''$)	B3P86	1.9740	1.1253	173.1	80.6	2.2283	1.1438	164.6
(B)	BHLYP	2.0290	1.1080	176.0	78.7	2.3447	1.1293	164.7
	B3PW91	1.9827	1.1256	173.4	80.8	2.2518	1.1442	164.6
	MP2(fc)	2.0612	1.1336	176.9	77.5	2.4807	1.1489	166.5
	MP2(fu)	2.0549	1.1329	176.9	77.5	2.4704	1.1482	165.8
species	method	Si−C	C−O	∠SiCO	∠OSiO	Si−O	O−C	∠SiOC
$Si(OC)_2^+$	B3LYP				84.7	2.3486	1.1419	175.1
($^2B_1$)	B3P86				83.0	2.2673	1.1426	173.1
(C)	BHLYP				81.8	2.3633	1.1282	173.5
	B3PW91				83.8	2.2941	1.1430	173.7
	MP2(fc)				78.6	2.4734	1.1496	177.8
	MP2(fu)				78.7	2.4679	1.1483	177.8
species	method	Si−C	C−O	∠SiCO	∠CSiC	Si−C	C−O	∠SiCO
$COSiCO^+$	B3LYP	2.0195	1.1241	181.4	91.8	2.9812	1.1317	78.0
($^2A''$)	B3P86	1.9889	1.1237	185.1	93.5	2.8543	1.1330	74.6
(TS1)	BHLYP	2.0691	1.1057	185.1	93.9	2.8901	1.1332	75.0
	B3PW91	1.9985	1.1239	180.0	87.7	2.9909	1.1169	84.5
	MP2(fc)	2.0933	1.1326	179.9	87.6	3.1319	1.1434	78.0
species	method	Si−O	C−O	∠SiOC	∠OSiC	Si−C	C−O	∠SiCO
$COSiCO^+$	B3LYP	2.2108	1.1544	176.0	88.1	2.7611	1.1422	79.9
($^2A''$)	B3P86	2.1786	1.1536	171.3	84.8	2.4439	1.1462	83.1
(TS2)	BHLYP	2.2162	1.1400	180.0	93.0	2.9983	1.1258	81.1
	B3PW91	2.2000	1.1537	176.9	85.6	2.5104	1.1468	80.1
	MP2(fc)	2.3264	1.1616	179.8	91.4	3.0951	1.1539	76.1

doublet state using four DFT (B3LYP, B3P86, B3PW91, and BHLYP) methods and MP2 with the 6-311+G* basis set. The results reveal that there are three isomers ($Si(CO)_2^+$ $^2B_1$, $COSiCO^+$ $^2A''$, and $Si(OC)_2^+$ $^2B_1$) on the global potential energy surface. All geometrical parameters, Mülliken charge populations, and harmonic frequencies are given in Tables 1−3, respectively. The transition state search has found two transition states for the isomerizations among three isomers. The optimized geometrical parameters, Mülliken charge populations, and vibrational frequencies for the transition states are also given in Tables 1−3. The corresponding zero-point vibrational energies (ZPVEs) for all these species are collected in Table 3. The stable isomers and the transition states have also been displayed in Figure 1. Table 4 lists the calculated total energies (E_T's) of the most stable isomer ($Si(CO)_2^+$ $^2B_1$), the energy separations of the other stable isomers, and the transition states relative to the most stable species. The adiabatic dissociation energies (D_e's) and the vertical electron affinities (EA_v's) of all isomers are given in Tables 5 and 6, respectively.

3.1. $Si(CO)_2^+$ Species. The geometrical optimizations have indicated that $Si(CO)_2^+$ ($^2B_1$) is the most stable species among the three isomers found on the global potential energy surface. The previous calculations on SiCO ($^3\Sigma^-$) in its triplet state reveal that the Si−CO binding energy is about ∼26 kcal/mol at several theoretical levels, while the preliminary examination predicts it for $SiCO^+$ ($^2\Pi$) cation to be 21.8 kcal/mol at the CCSD(T,full)/6-311+G* level. This observation has implied that in view of the bonding character of the SiCO ($^3\Sigma^-$) species it seemingly is more possible to form polycarbonyl Si^+ compounds. No experimental evidences have been reported so far for the existence of $Si(CO)_2^+$ ($^2B_1$). Only an early experiment demonstrated the existence of the bicarbonyl Si, $Si(CO)_2$ ($^1A_1$),

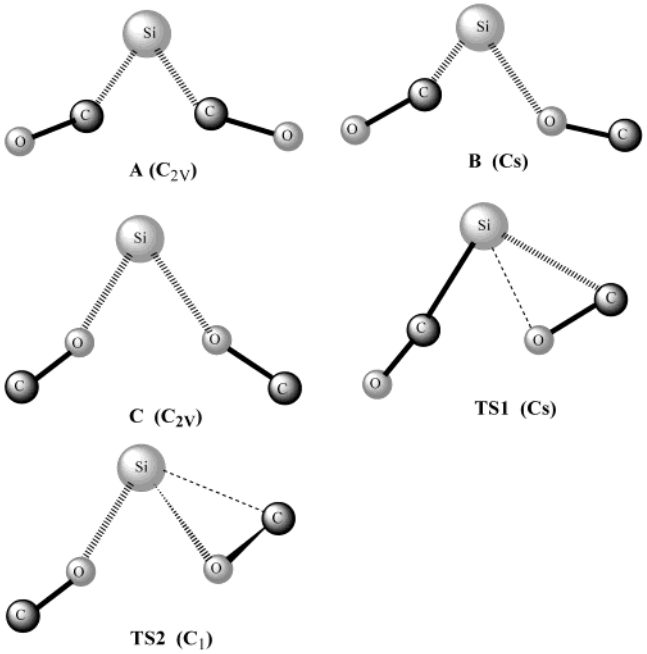

Figure 1. Structural diagrams of the optimized three isomers and two transition states of Si^+ binary carbonyl and isocarbonyl complexes.

TABLE 2: Calculated Partial Charge Distribution and Spin Densities for Three Isomers at the 6-311+G* Basis Set Level (ZPVE in kcal/mol)[a]

species	method	Q_{Si}	Q_C	Q_O	ρ_{Si}	ρ_C	ρ_O	ZPVE
$Si(CO)_2^+$	B3LYP	0.686	0.132	0.025	0.671	0.061	0.104	9.5656
$^2B_1$	B3P86	0.644	0.147	0.030	0.672	0.053	0.111	9.7665
(A)	BHLYP	0.665	0.178	−0.010	0.745	0.026	0.101	9.9270
	B3PW91	0.627	0.163	0.024	0.683	0.049	0.110	9.7357
	MP2(fc)	0.605	0.257	0.059	0.884	0.117	0.175	9.6615
	MP2(fu)	0.605	0.256	−0.059	0.882	−0.117	0.176	9.6871
$COSiCO^+$	B3LYP	0.761	0.099	0.036	0.782	0.126	0.112	8.1705
$^2A''$			0.052	0.051		0.013	−0.033	
(B)	B3P86	0.712	0.111	0.043	0.773	0.129	0.120	8.3420
			−0.011	0.144		0.019	−0.041	
	BHLYP	0.745	0.160	0.000	0.867	0.071	0.097	8.4997
			0.073	0.022		0.007	−0.042	
	B3PW91	0.700	0.132	0.038	0.786	0.123	0.124	8.3008
			−0.018	0.148		0.017	0.116	
	MP2(fc)	0.702	0.269	−0.054	1.000	−0.055	0.122	7.8755
			0.131	−0.047		−0.002	−0.065	
	MP2(fu)	0.701	0.266	−0.053	0.998	−0.054	0.124	7.9141
			0.130	−0.045		−0.002	−0.066	
$Si(OC)_2^+$	B3LYP	0.836	0.046	0.036	1.050	0.013	−0.038	7.2232
$^2B_1$	B3P86	0.789	−0.015	0.121	1.050	0.020	−0.045	7.3043
(C)	BHLYP	0.837	0.069	0.013	1.080	0.005	−0.045	7.5516
	B3PW91	0.798	−0.024	0.125	1.062	0.016	−0.047	7.2895
	MP2(fc)	0.852	0.120	−0.046	1.142	−0.005	−0.066	7.0277
	MP2(fu)	0.850	0.119	−0.044	1.143	−0.005	−0.067	7.0391
$COSiCO^+$	B3LYP	0.733	0.146	0.045	0.792	0.118	0.102	7.7154
$^2A''$			0.003	0.073		−0.006	−0.005	
(TS1)	B3P86	0.672	0.169	0.051	0.778	0.125	0.111	7.8682
			−0.014	0.121		−0.000	−0.006	
	BHLYP	0.879	0.201	0.006	0.879	0.055	0.080	8.0842
			0.014	0.042		−0.010	−0.004	
	B3PW91	0.665	0.187	0.047	0.789	0.119	0.107	7.8203
			−0.024	0.124		−0.009	−0.007	
	MP2(fc)	0.711	0.296	−0.005	0.975	−0.059	0.110	
			0.094	−0.051		−0.014	−0.011	
$COSiCO^+$	B3LYP	0.770	0.378	−0.250	0.963	0.027	−0.012	6.9095
$^2A''$			0.238	−0.136		0.026	−0.003	
(TS2)	B3P86	0.781	0.384	−0.256	0.895	0.028	−0.014	7.0391
			0.217	−0.126		0.093	−0.003	
	BHLYP	0.819	0.414	−0.303	0.996	0.018	−0.011	7.3230
			0.260	−0.190		−0.005	0.002	
	B3PW91	0.780	0.381	−0.255	0.915	0.025	−0.014	6.9601
			0.225	−0.132		0.076	−0.003	
	MP2(fc)	0.882	0.501	−0.430	1.006	0.010	−0.012	
			0.350	−0.304		−0.004	0.000	

[a] The first line is referred to the left SiCO or SiOC fragment, while the second line is referred to the right SiCO or SiOC fragment.

assigned from a slightly weak band at 1928 cm^{-1}.[19] They predicted this molecule to be linear, but no detailed IR vibrational analysis was given. Actually, the linear assignment for the $Si(CO)_2$ ($^1A_1$) molecular geometry lacks sufficient evidence. In 1989, Grev and Schaefer made a reassignment for the structure of $Si(CO)_2$ ($^1A_1$) on the basis of theoretically predicted IR spectra.[23] At the CISD/DZP level, they optimized three assumed structures for the $Si(CO)_2$ ($^1A_1$) species and indicated that the linear OCSiCO structure did not correspond to the minimum on the potential energy surface, and the ground state corresponded to a V-type structure. This V-type structure was verified by comparing the calculated frequencies with the experimental findings by Weltner and co-workers.[19] The predicted linear OCSiCO structure is significantly higher by 80.5 kcal/mol than the V-type structure at the CISD/DZP level.

However, whether the $Si(CO)_2^+$ ($^2B_1$) has similar structural character to that of its neutral species or not needs to be further investigated. In view of the lack of some information regarding structures and properties in the doublet state, in this section, the $Si(CO)_2^+$ ($^2B_1$) species will be deeply investigated at the DFT and MP2 levels with a larger basis set.

At six theoretical levels, the molecular geometries are first optimized for the $Si(CO)_2^+$ $^2B_1$ species in its doublet state. Optimizations indicate that the $Si(CO)_2^+$ $^2B_1$ state species possesses a bending structure (the V-type structure with C_{2v} symmetry). As occurred in the $Si(CO)_2$ $^3\Sigma^-$ state, not only is the C−Si−C unit of $Si(CO)_2^+$ ($^2B_1$) not linear, but also both of the two Si−C−O units are not linear. The linear structure only corresponds to a second-order saddle point with a couple of degenerate imaginary modes. In addition to $Si(CO)_2^+$ $^2B_1$ species, two other isomers have also been found ($COSiCO^+$ $^2A''$ and $Si(OC)_2^+$ $^2B_1$). These two species are energetically higher than the isomer $Si(CO)_2^+$ ($^2B_1$) by 22.77 and 40.89 kcal/mol at the CCSD(t,full)/6-311+G* level, respectively. Therefore, $Si(CO)_2^+$ ($^2B_1$) may be assigned to the most stable isomer on the global potential energy surface. This section mainly aims at $Si(CO)_2^+$ ($^2B_1$) species. The latter two isomers will be discussed in the following sections.

For the most stable state $Si(CO)_2^+$ ($^2B_1$) isomer, from the data in Table 1, it can be known that the key apex angle ∠CSiC reflecting the molecular nonlinear character is only ∼81° at six theoretical levels with the 6-311+G* basis set. It is slightly

TABLE 3: Optimized Harmonic Frequencies (in cm^{-1}) for Three Isomers and Two Transition States at the 6-311+G* Basis Set Level

species	methods	ω_1	ω_2	ω_3	ω_4	ω_5	ω_6	ω_7	ω_8	ω_9
		A_1	B_1	B_2	A_2	A_1	B_2	A_1	B_2	A_1
$Si(CO)_2^+$	B3LYP	101.2	266.2	304.1	316.4	352.5	405.2	548.5	2176.9	2220.2
$^2B_1$	B3P86	101.3	273.1	314.0	324.1	382.1	438.8	565.2	2196.0	2237.1
(A)	BHLYP	105.9	279.9	308.7	321.2	333.0	366.3	549.1	2318.9	2366.9
	B3PW91	100.9	271.7	312.1	322.9	376.7	434.7	561.7	2194.6	2234.8
	MP2(fc)	103.9	268.9	299.8	314.5	345.7	395.6	536.9	2232.3	2260.8
	MP2(fu)	103.3	271.1	301.0	317.3	348.0	397.7	538.8	2234.9	2264.0
species	methods	ω_1	ω_2	ω_3	ω_4	ω_5	ω_6	ω_7	ω_8	ω_9
		A′	A″	A′	A′	A″	A′	A′	A′	A′
$COSiCO^+$	B3LYP	77.6	138.8	150.2	169.4	253.4	289.9	380.1	2081.2	2174.7
$^2A''$	B3P86	80.8	145.4	163.3	190.4	257.4	310.9	417.0	2077.1	2192.9
(B)	BHLYP	79.2	137.6	151.8	167.6	262.3	278.6	342.9	2196.4	2329.3
	B3PW91	81.0	144.8	160.1	183.3	257.3	305.5	406.8	2076.5	2191.3
	MP2(fc)	68.3	109.2	129.2	144.8	241.6	256.1	368.4	2068.6	2186.5
	MP2(fu)	69.6	114.2	132.1	142.8	245.9	259.8	312.2	2072.7	2188.7
species	methods	ω_1	ω_2	ω_3	ω_4	ω_5	ω_6	ω_7	ω_8	ω_9
		A_1	B_2	A_1	A_2	B_1	B_2	A_1	B_2	A_1
$Si(OC)_2^+$	B3LYP	48.2	110.8	117.5	123.7	127.2	149.8	199.9	2082.8	2092.8
$^2B_1$	B3P86	57.2	114.3	124.8	130.3	132.1	163.3	218.6	2078.9	2089.8
(C)	BHLYP	49.9	110.5	119.7	119.9	125.0	149.7	198.4	2199.0	2210.5
	B3PW91	55.7	116.5	123.9	130.9	132.9	157.5	212.6	2097.2	2089.8
	MP2(fc)	47.6	103.8	118.6	104.3	108.2	134.6	171.8	2061.6	2065.5
	MP2(fu)	46.5	102.7	118.0	104.1	108.4	135.1	172.3	2066.4	2070.4
species	methods	ω_1	ω_2	ω_3	ω_4	ω_5	ω_6	ω_7	ω_8	ω_9
$COSiCO^+$	B3LYP	189.9i	25.8	68.7	103.7	250.1	251.4	339.4	2168.6	2189.3
$^2A''$	B3P86	201.2i	18.3	81.6	133.0	255.8	269.6	380.5	2161.9	2203.3
(TS1)	BHLYP	187.8i	44.5	68.0	93.3	249.6	258.4	281.7	2300.0	2359.5
	B3PW91	199.5i	20.5	77.6	119.8	253.6	263.3	369.8	2162.3	2203.5
species	methods	ω_1	ω_2	ω_3	ω_4	ω_5	ω_6	ω_7	ω_8	ω_9
$COSiCO^+$	B3LYP	191.8i	14.9	47.5	94.5	131.6	137.2	200.9	2062.2	2144.5
$^2A''$	B3P86	155.8i	57.2	84.5	117.7	137.2	161.9	217.7	2067.2	2080.4
(TS2)	BHLYP	192.1i	40.0	46.7	94.1	125.4	127.8	198.0	2184.0	2305.5
	B3PW91	147.2i	57.2	75.1	90.0	132.9	146.8	209.6	2069.3	2087.7

TABLE 4: Total Energies (E_T, au) of the Ground State Species ($Si(CO)_2^+$) and the Energy Separations (ΔE, kcal/mol) of the Other Two Isomers and the Two Transition States Relative to the Ground State

method	E_T(A)	ΔE(B)	ΔE(C)	ΔE(B)[a]	ΔE(C)[a]	ΔE(TS1)	ΔE(TS2)
B3LYP	−515.885 5981	21.21	37.95	19.82	35.61	28.58	45.74
B3P86	−516.597 3062	25.08	45.05	23.65	42.59	33.07	52.61
BHLYP	−515.742 9792	16.74	28.81	15.32	26.44	24.84	36.96
B3PW91	−515.732 9505	24.94	44.62	23.50	42.17	32.49	52.13
MP2[b]	−514.849 4177	23.03	38.83	21.24	36.20	34.43	44.97
MP3[b]	−514.835 8140	17.41	29.02	15.62	26.39	29.58	36.91
MP4SDQ[b]	−514.863 9096	16.88	28.89	15.09	26.26	28.73	36.00
CCSD(T)[b]	−514.892 4519	17.62	30.71	15.83	28.08	29.62	37.61
MP2[c]	−515.048 8680	23.25	39.18	21.48	36.53		
MP3[c]	−515.036 5777	17.56	29.24	15.78	26.60		
MP4SDQ[c]	−515.064 4585	17.00	29.10	15.23	26.45		
CCSD(T)[c]	−515.094 2735	17.84	31.09	16.07	28.45		
MP2[d]	−515.125 9054	27.68	47.97	25.03	46.20		
MP3[d]	−515.115 0334	22.33	38.91	19.68	37.13		
MP4SDQ[d]	−515.135 2631	21.64	38.45	18.99	36.68		
CCSD(T)[d]	−515.175 4648	22.77	40.89	20.13	39.11		

[a] The corrected energy separations by the zero-point vibrational energies. [b] The full-electron correlation calculations with the 6-311+G* basis set on the basis of MP2(fc)/6-311+G* geometries. [c] The full-electron correlation calculations with the 6-311+G* basis set on the basis of MP2(full)/6-311+G* geometries. [d] The full-electron correlation calculations with the aug-cc-pvtz basis set on the basis of MP2(full)/6-311+G* geometries.

larger than that (75−79°) of the corresponding neutral $Si(CO)_2$ ($^1A_1$) species at the same levels.[33] Another very interesting bond angle is ∠SiCO. At six theoretical levels, its optimized values are 167.0−168.4°, and are slightly smaller that those (170−171°) of the corresponding neutral species $Si(CO)_2$ ($^1A_1$). This molecule possesses C_{2v} symmetry; two SiCO moieties are symmetrically laid on the two sides of the C_2 axis, and every O atom bent of the Si−C axis by about 13° on the outside. Obviously, these DFT results for the angles are in good agreement with those calculated at the MP2 levels both with and without the inner-shell electron correlation. The optimized C−O bond lengths are within 1.11−1.13 Å, also exhibiting a

TABLE 5: Adiabatic Dissociation Energies (D_e, in kcal/mol) of Three Stable Isomers Calculated with the 6-311+G* Basis Set and Various Methods[a]

method	$D_{e,1}$(A)	$D_{e,2}$(A)	$D_{e,1}$(B)	$D_{e,1'}$(B)	$D_{e,2}$(B)	$D_{e,1}$(C)	$D_{e,2}$(C)
B3LYP	30.55	57.28	9.33	24.91	36.07	8.17	19.33
B3P86	36.00	66.71	10.92	29.09	41.63	9.12	21.66
BHLYP	26.44	48.35	9.69	20.60	31.60	8.53	19.53
B3PW91	34.65	64.28	9.71	27.84	39.35	8.16	19.67
MP2[b]	30.41	53.85	7.38	23.08	30.82	7.28	15.03
MP3[b]	25.69	45.70	8.28	19.45	28.29	7.84	16.68
$MP4_{SDQ}$[b]	24.79	45.15	7.91	19.71	28.27	7.70	16.26
CCSD(T)[b]	26.22	47.76	8.60	21.14	30.15	8.05	17.05
MP2[c]	30.82	54.54	7.57	23.37	31.29	7.45	15.36
MP3[c]	26.03	46.27	8.47	19.71	28.72	8.02	17.03
$MP4_{SDQ}$[c]	25.07	45.63	8.07	19.94	28.62	7.84	16.53
CCSD(T)[c]	26.61	48.43	8.77	21.45	30.59	8.20	17.34

[a] All these energy data are uncorrected by the zero-point vibrational energies and BSSE. The dissociation schemes for every species are defined here: A, $Si(CO)_2^+ \rightarrow SiCO^+ + CO$ ($D_{e,1}$(A)), $Si(CO)_2^+ \rightarrow Si^+ + 2CO$ ($D_{e,2}$(A)); B, $COSiCO^+ \rightarrow SiCO^+ + CO$ ($D_{e,1}$(B)), $COSiCO^+ \rightarrow SiOC^+ + CO$ ($D_{e,1'}$(B)), $COSiCO^+ \rightarrow Si^+ + 2CO$ ($D_{e,2}$(B)); C, $Si(OC)_2^+ \rightarrow SiOC^+ + CO$ ($D_{e,1}$(C)), $Si(OC)_2^+ \rightarrow Si^+ + 2CO$ ($D_{e,2}$(C)). [b] The frozen-core electron correlation calculations on the basis of MP2(fc)/6-311+G* geometries. [c] The full-electron correlation calculations on the basis of MP2(full)/6-311+G* geometries.

TABLE 6: Vertical Electron Affinities (EA_v, in kcal/mol) of Three Stable Isomers Calculated with the 6-311+G* Basis Set and Various Methods[a]

method	EA_v(A)	EA_v(B)	EA_v(C)
B3LYP	182.80	164.95	144.89
B3P86	197.71	178.53	157.25
BHLYP	174.40	156.49	137.27
B3PW91	184.54	165.45	144.34
MP2[b]	167.71	149.88	133.34
MP3[b]	169.82	151.47	132.48
$MP4_{SDQ}$[b]	167.41	151.25	134.69
CCSD(T)[b]	169.90	152.95	136.23
MP2[c]	168.01	150.18	133.34
MP3[c]	169.95	151.60	132.39
$MP4_{SDQ}$[c]	167.52	151.32	134.53
CCSD(T)[c]	170.09	153.11	136.09

[a] All these energy data are uncorrected by the zero-point vibrational energies and BSSE. [b] The frozen-core electron correlation calculations on the basis of MP2(fc)/6-311+G* geometries. [c] The full-electron correlation calculations on the basis of MP2(full)/6-311+G* geometries.

good agreement among four DFT and two MP2 methods. These C−O bond lengths are slightly shorter than those (1.15−1.16 Å) in the neutral species $Si(CO)_2$ ($^1A_1$). The Si−C bond lengths fall within 1.934−1.976 Å. They are obviously longer than those of the $Si(CO)_2$ ($^1A_1$) species by 0.12−0.15 Å at the same levels. Compared with those of the monocarbonyl $SiCO^+$ ($^2\Pi$) (Si−C, 2.004−2.101 Å; C−O, 1.105−1.132 Å), the Si−C bond lengths in $Si(CO)_2^+$ ($^2B_1$) are slightly shorter by 0.07−0.10 Å, while those for the C−O bond are almost equivalent. The largest deviation between the monocarbonyl and bicarbonyl Si^+ lies in the ∠SiCO angle. The difference is about 13°. Obviously, this phenomenon should be attributed to the break of a weak π bonding (there are two weak π bondings for SiCO, but there is only one for each SiCO molecular fragment in $Si(CO)_2^+$ ($^2B_1$)).

Obviously, these considerable changes should be due to the difference between them in the bonding character. The frontier orbital valence electronic configuration of the $Si(CO)_2^+$ ($^2B_1$) state is [core]...$(1b_1)^2(4a_1)^2(1a_2)^2(4b_2)^2(5a_1)^2(2b_1)^1(6a_1)^0$. Compared with the corresponding neutral species, this electronic state is yielded by ionizing an electron from the $2b_1$ orbital of the $Si(CO)_2$ $^1A_1$ state (...$(5a_1)^2(2b_1)^2(6a_1)^0$) or that from the $6a_1$ orbital of the $Si(CO)_2$ $^3B_1$ state (...$(5a_1)^2(2b_1)^1(6a_1)^1$). The main distinction between the electronic configurations of $Si(CO)_2$ ($^1A_1$) and $Si(CO)_2^+$ ($^2B_1$) is the different occupation of the highest-occupied molecular orbital (HOMO). Therefore, the HOMO interaction character has directly determined the structure and property of $Si(CO)_2^+$ ($^1A_1$) and its difference from

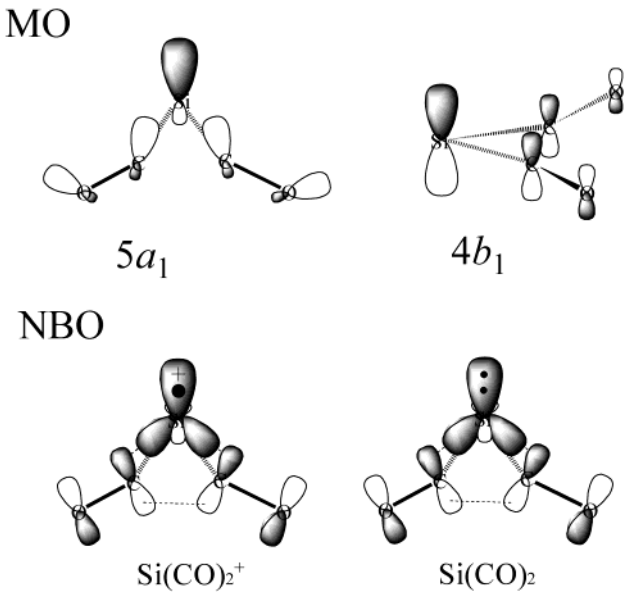

Figure 2. Bonding molecular orbital (MO) interaction diagram for $Si(CO)_2^+$ and natural bonding orbital (NBO) interaction comparison between $Si(CO)_2$ and $Si(CO)_2^+$ species.

$Si(CO)_2$ ($^1A_1$). Inspection of the high-energy-level bonding orbitals reveals that the HOMO ($2b_1$) denotes the interaction of the Si π-type p orbital with the antibonding π^* orbital of CO and mainly reflects the π-bonding interaction between Si and C centers and the π^*-antibonding interaction between C and O centers. In addition, several other interaction bonds of interest are $4a_1$, $1a_2$, $4b_2$, and $5a_1$ orbitals. $4a_1$ and $1a_2$ depict the σ-bonding and π-bonding interaction localizing at the CO moiety, respectively, while $4b_2$ corresponds to the σ^* antibonding interaction between C and O centers, and the $5a_1$ is the Si−C σ-bonding orbital. Obviously, the key molecular orbitals describing the bonding interaction between Si and CO moieties are $5a_1$ and $2b_1$ for the $Si(CO)_2^+$ $^2B_1$ state (cf. Figure 2). From the electronic configuration of $Si(CO)_2$ ($^1A_1$) it should be known that the electron ionization from the $2b_1$ orbital should weaken the Si−C bond and strengthen the C−O bond, resulting in that the Si−C bond should be elongated and the C−O bond should be shortened. This prediction is true for $SiCO/SiCO^+$ and $Si(CO)_2/Si(CO)_2^+$ systems, but the change amount is larger for the former than that for the latter. The C−O bond lengths in both $SiCO^+$ ($^2\Pi$) and $Si(CO)_2^+$ ($^2B_1$) are very close to those of the free state CO molecule. This tendency has indicated that in

the π-type HOMO the occupying electron comes from the Si π-type p orbital electron. Removing this electron causes CO to be recovered as its free state orbital interaction character. The charge population (Si: +0.6 e) and the spin density distribution (0.67−0.88) given in Table 2 have also verified this prediction.

Another interesting character for these $Si(CO)_2^+$ ($^2B_1$) is that there are a very small ∠CSiC bond angle and the slight bending ∠SiCO bond angle. This structural character is to some extent similar to that in the silenes such as H_2Si and so forth but is different from that in SiCO ($^3\Sigma^-$), $SiCO^+$ ($^2\Pi$) species and some transition metal carbonyl compounds. For H_2Si species, the ground state is the singlet state $^1A_1$ state, and its ∠HSiH bond angle is about 91°, while, for H_2Si^+ species, the ∠HSiH bond angle in its doublet state is about 120°. For the $Si(CO)_2^+$ ($^2B_1$) cation, the ∠CSiC angle (∼81°) is also larger than that (∼77°) of the neutral $Si(CO)_2$ ($^1A_1$) species. Obviously, $Si(CO)_2^+$ ($^2B_1$) may be classified as the silene, but there is some difference between them in the bonding of interest. This difference is certainly attributed to the participation of CO as ligand. Inspection of the natural bond orbital (NBO, cf. Figure 2) reveals that, for the most stable state species ($Si(CO)_2^+$ $^2B_1$), Si utilizes two hybrid orbitals ($sp^{16.55}d^{0.30}$) to interact with two C ($sp^{0.6}$) hybrid orbitals to form two Si−C bonds. In these two hybrid orbitals of Si in $Si(CO)_2^+$ ($^2B_1$), the p orbital component is larger than that of ($sp^{7.53}d^{0.13}$) in the $Si(CO)_2$ ($^1A_1$) species. A similar situation also exists for H_2Si and H_2Si^+ systems. Obviously, if Si uses its pure p orbitals to form Si−C bonds, the ∠CSiC angle should be 90°. However, according to the hybrid orbital principle, the p orbital component (92.7%) in the present species is smaller than 100% (the pure p orbital) and larger than that (66.7%) in the sp^2 hybrid orbital; thus, the ∠CSiC angle should be larger than 90° and smaller than 120°. But the ∠CSiC in the present system is only about 81°, and still smaller than the pure p orbital angle. Obviously, this bonding interaction character may not be interpreted. Of course, the repulsion interaction from a pair of lone electrons of Si also takes a part in forcing the ∠CSiC angle to become small, but this repulsion interaction is not strong enough to make the ∠CSiC angle smaller than 90°; moreover, the center atom Si^+ is a monovalent cation. In addition, for H_2Si and H_2Si^+ species, removing an electron from H_2Si results in the ∠HSiH angle (120°) in H_2Si^+ becoming larger than that (91°) in H_2Si. This obviously is reasonable, because the repulsion interaction from the lone electron in the H_2Si^+ species is smaller than that in H_2Si; the former has only one lone electron, while the latter has a pair of lone electrons. But for these systems, although removing an electron from $Si(CO)_2$ ($^3\Sigma^-$) also causes its ∠CSiC angle to become small, the change magnitude is smaller than that in the H_2Si and H_2Si^+ cases. And the ∠CSiC angle is still smaller than 90°. Therefore, it can be predicted that the bonding must be different from that in H_2Si and common hydrocarbon compounds. Actually, for the present system, the difference from that in the H_2Si^+/H_2Si case mainly comes of the difference of carbonyl from hydrogen atom. In H_2Si, each H atom uses its 1s orbital with one electron to form covalent bonding with a singly occupied hybrid orbital of the Si center, while, in the present system, Si^+ uses its s orbital and in-plane two p orbitals to make up three unequivalent hybrid orbitals. Since these hybrid orbitals are energetically significantly higher than the CO lone-pair electron orbital and are close to the CO π^* orbitals, the linear combination with the CO lone-pair electron orbital is energetically less favorable than that with the CO π^* orbitals. Therefore, the bonding between Si and each CO should be the interaction between one unoccupied Si hybrid orbital and the CO in-plane π^* orbital. Obviously, if the combination between Si and C is the bonding, that between Si and O must be the antibonding. Therefore, in geometry the Si−O distance should be far loner than the Si−C distance, causing the ∠SiCO to be bent (∼167°). And the strong repulsion interaction coming from the lone electron also causes the ∠CSiC angle to be more bent than the ∠HSiH angle of H_2Si^+. Of course, it is also easy to explain such a fact that the ∠CSiC angle of $Si(CO)_2^+$ ($^2B_1$) is larger than that of $Si(CO)_2$ ($^3\Sigma^-$); this is because there is only one lone electron for the former and two lone electrons for the latter. In addition, another important aspect should also be taken into account. For the in-plane π^* orbitals of two CO moieties, the C positive phase parts of two C centers combine with Si hybrid orbitals, respectively, and their negative phase parts also interact with each other because they have the same orbital phase. Therefore, it can be concluded that the C−C interaction is also a predominant factor to cause the ∠CSiC angle to be smaller than 90°. Our optimized C−C bond distance of ∼2.57 Å has fully proved this analysis. Although there is also a $\pi^*-\pi^*$ long-range bonding coupling interaction between two −C═O molecules, the repulsion interaction between the lone electron pairs of two terminal O centers forces two O centers to part from each other. Perhaps this is why two terminal O atoms bent of the Si−C axis by ∼13° on the outside.

Table 3 collects the frequencies for nine possible vibrational modes (four A_1, one A_2, one B_1, and three B_2) obtained using six different theoretical methods. Obviously, ω_8 (B_2) and ω_9 (A_1) may be undoubtedly assigned to two C═O character absorption peaks with asymmetric and symmetric stretching vibrations, while ω_6 (B_2) and ω_7 (A_1) correspond to the Si−CO asymmetric and symmetric stretching vibrations. These two groups of vibrational modes reflect the strength of the corresponding bonds, respectively. Another vibrational mode of interest is the ω_1 (A_1) mode, which denotes the bending vibration of the ∠CSiC angle. The remaining modes are in-plane bending vibrational modes (ω_3, B_2 and ω_5, A_1) and out-of-plane waggle modes (ω_2, B_1 and ω_4, A_2) for the ∠SiCO angle. As noted in the analysis concerning geometric parameters, very good agreement among data obtained using several theoretical methods can also be observed except for BHLYP (viz. BHandHLYP). This BHLYP method seemingly overestimates ω_8 and ω_9 values. Further, a very interesting observation is the changes of the vibrational frequencies for the C−O stretching mode. Comparing $Si(CO)_2^+$ ($^2B_1$) with $SiCO^+$ ($^2\Pi$), the C−O bond length change and C−O stretching frequency change are small; they are close to those of the free state CO ($^1\Sigma$) molecule. But comparing them with corresponding neutral species ($Si(CO)_2$ $^1A_1$ state), the decrease of the C−O bond lengths and the increase of the C−O stretching frequencies are not negligible, being about 0.02−0.03 Å and 170−270 cm^{-1}, respectively. These considerable variations indicate that the weakening of the C═O bonds in $Si(CO)_2^+$ ($^2B_1$) is smaller than that in the monocarbonyl Si^+, and also smaller than that in $Si(CO)_2$ ($^1A_1$). The CO of $Si(CO)_2^+$ ($^2B_1$) possesses the free state CO molecular character. From this we can predict whether the CO moieties in polycarbonyl Si^+ such as $Si(CO)_3^+$ or $Si(CO)_4^+$ and so forth are essentially closer to the free state CO ($^1\Sigma^+$). It should be possible, but the bonding interaction is too weak for these kinds of polycarbonyl Si^+ (or Si) compounds to stably exist. Perhaps this is why there are no experimental reports regarding the existence of the tricarbonyl Si or other polycarbonyl Si complexes, even of polycarbonyl Si^+ with more than two carbonyls. In addition, the Si−C vibrational frequencies (ω_6, ω_7) in $Si(CO)_2^+$ ($^2B_1$) are smaller than those in the neutral

$Si(CO)_2$ $^1A_1$ state by 100−160 cm^{-1}, while the angle ∠CSiC bending vibrational frequency is almost unchanged. However, the ω_6 and ω_7 of $Si(CO)_2^+$ ($^2B_1$) are significantly larger than the Si−C stretching frequency of $SiCO^+$ ($^2\Pi$). This tendency has reflected that the average strength of the Si−C bond of $Si(CO)_2^+$ ($^2B_1$) is stronger than that in $SiCO^+$ ($^2\Pi$) and weaker than that in $Si(CO)_2$ ($^1A_1$), and $Si(CO)_2^+$ ($^2B_1$) does still belong to the weak interaction system. The small value for ∠CSiC bending has also implied the above analysis that the bonding interaction between Si^+ and two CO is weak, and the potential energy surface is flat with respect to the bending vibration of the angle ∠CSiC, and thus this bicarbonyl Si^+ molecule is facile.

To further check the bonding strength of this bicarbonyl Si^+ complex and to predict the stability of the polycarbonyl Si^+ complexes, the mono-carbonyl adiabatic dissociation energies and the bi-carbonyl adiabatic dissociation energies and the corresponding vertical electron affinities of the $Si(CO)_2^+$ $^2B_1$ state are also determined by using six methods with the 6-311+G* basis set, and are also calibrated by the higher level electron correlation methods such as MP3, $MP4_{SDQ}$, and CCSD(T) (see Tables 5 and 6). No reports have been given elsewhere for the investigations about these energy quantities. Therefore, the analysis will be limited to explore the intrinsic relationship between the bonding and relevant energy parameters at the theoretical level.

For the first CO dissociation energy, $D_{e,1}$, the B3P86 and B3Pw91 methods give $D_{e,1}$ within 34.6−36.0 kcal/mol, while the B3LYP method gives the $D_{e,1}$ value 30.6 kcal/mol. The latter result is very close to the two MP2 ones (30.4 and 30.8 kcal/mol). At the high electron correlation levels, the MP3, $MP4_{SDQ}$, and CCSD(T) methods give them within 24.8−26.6 kcal/mol, and are fortunately in good agreement with the BHLYP value (26.4 kcal/mol). They are slightly smaller than those at the B3LYP level and the two MP2 levels, and are significantly smaller than the B3P86 and B3PW91 results. According to the performances of various methods, the results falling within 26−30 kcal/mol are reliable. Comparison of these values with those of $SiCO^+$ ($^2\Pi$) indicates that the first CO adiabatic dissociation energy is greater than the second CO adiabatic dissociation energy, viz., the CO adiabatic dissociation energy of $SiCO^+$ ($^2\Pi$), by 4−7 kcal/mol at several different levels. Namely, the dissociation of $Si(CO)_2^+$ ($^2B_1$) into $SiCO^+$ ($^2\Pi$) and CO ($^1\Sigma^+$) is slightly more difficult than that of $SiCO^+$ ($^2\Pi$) into Si^+ (^2P) and CO ($^1\Sigma^+$). In other words, it is to say that the first CO binding energy of Si^+ ion is smaller than the second CO one. This tendency is inverse to that in the $Si(CO)_2$ ($^1A_1$) system, in which the first CO binding energy of Si is greater than the second CO one. By extending this tendency, it may be predicted that the third CO binding energy of Si^+ should be greater than the second CO one, and the same should be true for the fourth or fifth CO binding energies. This prediction indicates that there should exist the tricarbonyl Si^+. But, up to now, no confirmed reports have been given elsewhere for the existence of the polycarbonyl Si^+ with more than two carbonyls both in theoretical and experimental aspects. However, if making an analysis from the viewpoint of averaged single CO binding energy, another conclusion may be drawn. The averaged value (24.2 kcal/mol at the CCSD(T)/6-311+G* level) for the $Si(CO)_2^+$ species is very close to that (21.8 kcal/mol at the same level) for the $SiCO^+$ ($^2\Pi$) species, and is also very close to that (22.8 kcal/mol) for the $Si(CO)_2$ ($^3\Sigma^-$) species. This indicates that increasing a positive charge for $Si(CO)_2$ ($^3\Sigma^-$) cannot significantly improve its stability. In view of the bonding analysis mentioned above, it is easily predicted that if $Si(CO)_2^+$ ($^2B_1$) can combine another CO ligand, the center Si^+ must adopt an unequivalent sp^3 hybrid to form four unequivalent hybrid orbitals. Among them, one is occupied by a lone electron coming from the Si^+ center, and the other three are used to interact with the π^* orbitals of the three CO ligands. Obviously, for this situation, perhaps there is only the bonding between the Si^+ hybrid orbital and the π^* orbital of CO, but there surely is not the C···C interaction. The latter interaction is also very important for further stabilizing the system. Therefore, there must be a large repulsion interaction in this situation. The repulsion interaction among the three CO's would force the system to become planar, but the repulsion interaction from the lone electron to CO would force the system to become a pyramid. However, due to the weak ability of Si p and d orbitals for accepting electrons, the CO binding energy of Si^+ cannot significantly increase along with the increase of ligand CO number, and the third CO binding energy is smaller than the repulsion energy increased by introducing the third CO. Therefore, for the tricarbonyl Si^+ (if existing), it may be predicted that the average binding energy should be far smaller than that of $Si(CO)_2^+$ ($^2B_1$). This tendency has implied that polycarbonyl Si^+ complexes with more than two CO's should be metastable or unstable, and they are very easily dissociated into sub-carbonyl Si^+ complexes. This further confirms such a fact that up to now there have not been any reports regarding $Si(CO)_3^+$ or $Si(CO)_4^+$ and so forth even if at very low temperature. This is the same as the situation of polycarbonyl Si, although Si^+ ion has a positive charge and has a stronger ability for attracting electrons than Si atom.

Another important energy quantity is EA_v, the vertical electron affinity. Table 6 gives the relevant EA_v results calculated at several theoretical levels. Four DFT methods give EA_v within 174−197 kcal/mol with a slightly large deviation (∼17 kcal/mol), while several wave function-correlated methods (MP2, MP3, MP4, and CCSD) give the results (167−170 kcal/mol) very close to each other. Thus, it can be concluded that EA_v falling within 170−180 kcal/mol is reliable. Very interesting is that EA_v of $Si(CO)_2^+$ ($^2B_1$) is very close to that of Si^+ (186.7, 201.2, 190.5, and 179.2 kcal/mol at B3LYP, B3P86, B3PW91, and CCSD(T) with the 6-311+G* basis set, respectively). The corresponding difference between Si^+ EA_v and EA_v of $Si(CO)_2^+$ ($^2B_1$) is only 4−9 kcal/mol. Together with the charge population, this phenomenon has fully shown that the ionized electron mainly comes from the Si center, confirming $Si(CO)_2^+$ ($^2B_1$) to have the silene character.

3.2. $Si(OC)_2^+$ Species. Since the CO molecule has a very small dipole moment, it is not an electrostatics interactant. However, C and O are the same periodic elements; the C-terminal and O-terminal in the formed CO molecule also have similar structural character. Thus, from the bonding analysis about $Si(CO)_2^+$ ($^2B_1$) mentioned above, it can be predicted that CO may also interact with Si^+ ion by the O-terminal. Since the lone-pair electrons at the O-terminal are energetically lower than those at the C-terminal, it can be predicted that the interaction strength between Si^+ and CO by the O-terminal may be weaker than that by the C-terminal, and the formed complexes by the O-terminal are generally less stable than the corresponding ones by the C-terminal. But, $Si(OC)_2^+$ should have the same bonding character as $Si(CO)_2^+$ ($^2B_1$). The geometric optimizations have confirmed the above analysis. The $Si(OC)_2^+$ ($^2B_1$) also corresponds to a minimum on the global potential energy surface. The calculated results indicate that the $Si(OC)_2^+$ ($^2B_1$) is energetically higher by 28.8−45.1 kcal/mol than the $Si(CO)_2^+$ ($^2B_1$) at several different levels. For this energy separation,

different levels of theory give different results with the deviation of ~16 kcal/mol. B3P86 and B3PW91 methods yield the state−state energy separation 44.6−45.1 kcal/mol, but BHLYP gives the value only 28.8 kcal/mol, being close to the MP3 and MP4 results, at the same basis set level (6-311+G*). The B3LYP calculated value is 38.0 kcal/mol; it is very close to the MP2 values (~39.0 kcal/mol) at the different cases. Inclusion of the inner-shell electron correlation cannot improve the energy separation, but at the full-electron correlation level and on the basis of MP2(full)/6-311+G* geometries, the enlargement of the basis set from 6-311+G* to aug-cc-pvtz for single-point calculation may significantly increase the energy separation by ~9.0 kcal/mol. According to the performance of several methods, it can be believed that the energy separation of $Si(OC)_2^+$ ($^2B_1$) related to $Si(CO)_2^+$ ($^2B_1$) should be between 30 and 40 kcal/mol.

For this $Si(OC)_2^+$ ($^2B_1$) species, the optimized Si−O bond length is within 2.267−2.473 Å at six different levels. The results obtained using the B3LYP and BHLYP methods with the 6-311+G* basis set are very close to each other; they are slightly longer than those obtained at the B3P86/6-311+G* and B3PW91/6-311+G* levels, and slightly smaller than those obtained at the two MP2 levels with the same basis set. Compared with the Si−C bonds in $Si(CO)_2^+$ ($^2B_1$), the Si−O bonds in $Si(OC)_2^+$ ($^2B_1$) are significantly longer by 0.3−0.5 Å. They are also slightly longer by 0.05~0.09 Å than that of $SiOC^+$ ($^2\Pi$) at the same levels. These observations seemly give us a note that the Si−O bond in this system is weaker than the Si−C bond in the $Si(CO)_2^+$ system. Obviously, this prediction is reasonable, and it is also a full evidence for the above analysis about the relative stability. For the C−O bond, the calculated results fall within 1.128−1.149 Å. These values are slightly longer than those in the $Si(CO)_2^+$ ($^2B_1$) system, and are almost equivalent to those in the $SiOC^+$ ($^2\Pi$) species, indicating that the C−O bond in this species is also weaker than that in the $Si(CO)_2^+$ ($^2B_1$) species. The optimized apex angle ∠OSiO (79−84°) in $Si(OC)_2^+$ ($^2B_1$) is also equivalent to the ∠CSiC apex angle in $Si(CO)_2^+$ ($^2B_1$). However, the optimized ∠SiOC angle (173−177°) is slightly different from the ∠SiCO angle (~167°) in the $Si(CO)_2^+$ ($^2B_1$) species.

Compared with the case of the corresponding neutral species, $Si(OC)_2$ ($^1A_1$), there are significant differences between them for geometrical parameters. Although several theoretical methods have some different behaviors in predicting the geometric parameters of $Si(OC)_2$, ($^1A_1$), the relative regularity of the geometric parameter change agrees well with that found for the $Si(OC)_2^+$ ($^2B_1$) species. Namely, the value (2.532 Å) obtained by the B3LYP method is longer than those (2.125 and 2.231 Å) obtained by the B3P86 and BHLYP methods and is shorter than those (2.838 and 2.883 Å) obtained by the BHLYP and MP2 methods. The same regularity has also been found for SiOC ($^3\Sigma^-$ and $^1\Delta$) and $SiOC^+$ ($^2\Pi$) species. Obviously, the calculations on this kind of complexes with coordination by the O-terminal of the carbonyl (CO) have presented a serious challenge for theoreticians. We leave further studies concerning this problem for the theoretical experts who major in the method development. But, comparing the change of the Si−O bond of $SiOC^+$ ($^2\Pi$) relative to that of SiOC ($^3\Sigma^-$) and the cases occurring in $SiCO/SiCO^+$ and $Si(CO)_2/Si(CO)_2^+$, it could be believed that the Si−O bond of $Si(OC)_2^+$ ($^2B_1$) should be longer than that of $Si(OC)_2$ ($^1A_1$). Thus, the reliable Si−O bond lengths for $Si(OC)_2^+$ ($^2B_1$) should be 2.26−2.34 Å. This observation has indicated that adding an electron to the $Si(OC)_2^+$ ($^2B_1$) species may make the Si−O bond shorter. This is the same as that observed in the $Si(CO)_2^+$ ($^2B_1$) species. These same change tendencies for Si−O bonds have implied that $Si(OC)_2^+$ ($^2B_1$) has same bonding character as $Si(CO)_2^+$ ($^2B_1$). Although there exist some deviations for the Si−O bond length at several theoretical levels, they are obviously longer than the general Si−O bonds in the other Si−O bond-containing compounds. This observation has fully indicated that the bonding of Si^+ with the CO moiety by the O-terminal still belongs to the weak interaction no matter in the monocarbonyl Si^+ or in the dicarbonyl Si^+, and even they are weaker than the SiOC ($^3\Sigma^-$) and $Si(OC)_2$ ($^1A_1$) species. From the above analysis, it is also easily found that the electrostatic interaction is not dominant in this system; and the same is true for $Si(CO)_2^+$ ($^2B_1$) and the relevant monocarbonyl Si^+ species, although each species has an excess positive charge. This observation will also be confirmed by the following analysis about the frequency and bonding.

For this species, two important vibrational modes are still the ω_8 and ω_9 vibrations; they are assigned to the antisymmetric and symmetric stretching modes of the two C−O moieties in $Si(OC)_2^+$ ($^2B_1$). As occurred in the $Si(CO)_2^+$ ($^2B_1$) species, the symmetric stretching vibration is stronger than the antisymmetric one. Several methods have yielded the frequencies for these two modes very close to each other, except for the BHLYP method, which overestimated them by about 100 cm^{-1} for the antisymmetric mode and by 120 cm^{-1} for the symmetric mode. Compared with those of the $Si(CO)_2^+$ ($^2B_1$) species, these two frequencies are smaller by 90−120 cm^{-1} for ω_8 (B_2) and ~40 cm^{-1} for ω_9 (A_1). This observation has apparently shown that the Si−O bond in the $Si(OC)_2^+$ ($^2B_1$) species is weaker than that in the $Si(CO)_2^+$ ($^2B_1$) species, reflecting the consistency with the analysis about the bond lengths. This tendency is inverse to the case for the monocarbonyl species ($SiOC/SiOC^+$). Obviously, it is undoubted that these modes are also red-shifted relative to those of the isolated CO molecule. On the contrary, compared with those of the neutral $Si(OC)_2$ ($^1A_1$) species, these two vibrational modes are obviously blue-shifted by 120−160 cm^{-1} for ω_8 (B_2) and 80−130 cm^{-1} for ω_9 (A_1), indicating the strengthening of Si−O bonds in $Si(OC)_2^+$ ($^2B_1$) related to those in the $Si(OC)_2$ ($^1A_1$) species. Another important vibrational mode is ω_1 (A_1), which corresponds to the bending vibration of the ∠OSiO apex angle. The calculated bending frequency is within 46−57 cm^{-1} at the six theoretical levels used here. These values are apparently smaller than the ω_1 (A_1) ones (100−105 cm^{-1}) of the $Si(CO)_2^+$ ($^2B_1$) species, indicating that the potential energy surface for the ∠OSiO bending vibration of the $Si(OC)_2^+$ ($^2B_1$) species is much more flat than that of the $Si(CO)_2^+$ ($^2B_1$) species. It is also smaller than that of the corresponding neutral species, $Si(OC)_2$ ($^1A_1$). Thus it can be concluded that this molecule is much more flexible. However, this observation has presented us an interesting question: now that this small bending vibrational frequency has implied that the O−O coupling interaction seems impossible to exist, why is the ∠OSiO angle still so small? This question is left to be explained in the bonding analysis section.

Similarly, the ω_6 and ω_7 correspond to the Si−OC antisymmetric and symmetric stretching vibrations, respectively. Their values are within 135−157 cm^{-1} for ω_6 (B_2) and 171−218 cm^{-1} for ω_7 (A_1) at six different levels of theory, and are far smaller by 250−280 cm^{-1} for the ω_6 (B_2) mode and by ~150 cm^{-1} for the ω_7 (A_1) mode than the corresponding ones of the $Si(CO)_2^+$ ($^2B_1$) species. They are slightly greater than the corresponding ones of the neutral $Si(OC)_2$ ($^1A_1$) species. This phenomenon has verified again the above analysis that the Si−O bonds of

$Si(OC)_2^+$ ($^2B_1$) are weaker than those of the $Si(CO)_2^+$ ($^2B_1$) species, and are slightly stronger than those of the neutral $Si(OC)_2$ ($^1A_1$) species. Compared with the case of the monoisocarbonyl Si^+, the Si−OC stretching frequency in the $Si(OC)_2^+$ ($^2B_1$) species is also slightly smaller. This is in good agreement with the analysis from the Si−O bond length. The later discussion on the dissociation energies will also prove it to be correct. The other four frequencies correspond to the in-plane bending vibrational and the out-plane twist modes of the ∠SiOC angle. They also smaller than the corresponding ones of the $Si(CO)_2^+$ ($^2B_1$) species and that of the $SiOC^+$ ($^2\Pi$) species, but are slightly greater than and closer to those of the neutral $Si(OC)_2$ ($^1A_1$) species.

Obviously, the above-noted structural character should be closely related to the bonding and the interaction nature. The valence electronic configuration for the $Si(OC)_2^+$ ($^2B_1$) species is $[core]...(3b_2)^2(1b_1)^2(1a_2)^2(4b_2)^2(5a_1)^2(2b_1)^1(5b_2)^0$. It is the same as that of the $Si(CO)_2^+$ ($^2B_1$) species. Inspection of the character of these orbitals also exhibits the same bonding properties as those in the $Si(CO)_2^+$ ($^2B_1$) system. Namely, the HOMO ($2b_1$) denotes the interaction of the Si π-type p orbital with the antibonding π^* orbital of CO and mainly reflects the π-bonding interaction between Si and O centers and the π^*-antibonding interaction between O and C centers. In addition, several other interaction bonds of interest are the $4a_1$, $1a_2$, $4b_2$, and $5a_1$ orbitals. $4a_1$ and $1a_2$ depict the σ-bonding and π-bonding interaction localizing at the CO moiety, respectively, while $4b_2$ corresponds to the σ^*-antibonding interaction between the C and O centers, and the $5a_1$ is the Si−O σ-bonding orbital. The key molecular orbitals describing the bonding interaction between Si and OC moieties are also $5a_1$ and $2b_1$ for the $Si(OC)_2^+$ ($^2B_1$) species. The distinction between the orbitals of $Si(OC)_2^+$ ($^2B_1$) and those of $Si(CO)_2^+$ ($^2B_1$) is the bonding interaction of Si^+ with the CO molecule by the O-terminal instead of the C-terminal. Obviously, the above bonding analysis concerning the $Si(CO)_2^+$ ($^2B_1$) species may also be applicable to the $Si(OC)_2^+$ ($^2B_1$) species. Detailed comparison between the bonding orbitals of $Si(OC)_2^+$ ($^2B_1$) and those of the $Si(CO)_2^+$ ($^2B_1$) species reveals that the bonding orbital ($2b_1$) energy level in the $Si(OC)_2^+$ ($^2B_1$) species is higher by 27.62 kcal/mol than that in the $Si(CO)_2^+$ ($^2B_1$) species (−0.4431 au vs −0.4871 au at the B3P86/6-311+G* level). Perhaps this has implied why $Si(OC)_2^+$ ($^2B_1$) is less stable than the $Si(CO)_2^+$ ($^2B_1$) species.

Table 5 also lists the adiabatic dissociation energies for $Si(OC)_2^+$ ($^2B_1$) species. $D_{e,1}$ corresponds to the energy required for removing a CO from the $Si(OC)_2^+$ ($^2B_1$) system, while $D_{e,2}$ corresponds to that for removing two CO's from the $Si(OC)_2^+$ ($^2B_1$) system. At several theoretical levels, the calculated $D_{e,1}$ values are within 7.3−9.1 kcal/mol, and the DFT results are in good agreement with CCSD ones, but the MP2 values are slightly smaller than the others by 1.0−1.8 kcal/mol. The total dissociation energy, $D_{e,2}$, of the two carbonyls is within 16.1−19.6 kcal/mol, and the MP2 method slightly underestimates $D_{e,2}$, while the B3P86 method slightly overestimates it. From these two groups of data, one can extract the second carbonyl dissociation energy, viz., the dissociation energy of the $SiOC^+$ ($^2\Pi$) species, to be within 8.0−12.5 kcal/mol at six theoretical levels. Comparison has indicated that the first carbonyl dissociation energy is slightly smaller by 0.8−3.0 kcal/mol than the second carbonyl dissociation energy. This tendency is contrary to the case of the $Si(CO)_2^+$ ($^2B_1$) system. No matter what cases they are, these small dissociation energy values have undoubtedly shown that $Si(OC)_2^+$ ($^2B_1$) is less stable than $Si(CO)_2^+$ ($^2B_1$), and is much more easily dissociated into Si^+ and CO molecules; perhaps this is why no experimental reports have been found for the existence of the $Si(OC)_2^+$ ($^2B_1$) molecule ion. These dissociation energy data have also implied another impossibility about the existence of the polyisocarbonyl Si^+, such as $Si(OC)_3^+$ and so forth. In addition, the vertical electron affinity of the $Si(OC)_2^+$ ($^2B_1$) molecule listed in Table 6 has also given an additional remark for the weakness of the Si−O bonding. The calculated EA_v values fall within 132.5−144.9 kcal/mol with the deviation of about 12 kcal/mol (∼8.5%). These values reflect the stability of the system after accepting an electron. They are smaller by 34−40 kcal/mol than those of the $Si(CO)_2^+$ ($^2B_1$) species, indicating that the stabilization energy by accepting an electron of $Si(CO)_2^+$ ($^2B_1$) is larger than that of $Si(OC)_2^+$ ($^2B_1$), and $Si(CO)_2^+$ ($^2B_1$) will become more stable by accepting an electron. On the other hand, the greater the EA_v is, the stronger the oxidation ability is. The coordination of CO with the O-terminal to Si^+ may significantly reduce the oxidation ability of Si^+ ion much more than that with the C-terminal, and also considerably decrease the Si^+ Lewis acidity. This kind of complexity may prevent Si^+ or its subligand complexes from being further coordinated by other ligands.

In addition, it should be noted that the relative stability comparison of the $Si(OC)_2^+$ ($^2B_1$) species with the $Si(CO)_2^+$ ($^2B_1$) species has also confirmed CO to be a binucleophilic group; viz., with the O-terminal and the C-terminal nucleophilic sites, the nucleophilic ability of the C-terminal is far greater than that of the O-terminal. This observation agrees very well with the usual findings that CO is much more likely to form the carbonyl complexes by its C-terminal instead of the isocarbonyl ones by the O-terminal.

3.3. $COSiOC^+$ Species. The above analysis has confirmed the existence of bicarbonyl Si^+ and bi-isocarbonyl Si^+ molecules. Now that the CO molecule has the binucleophilic sites, the remaining question is whether the mixing carbonyl Si^+ species, viz., $COSiCO^+$, does exist. The answer should be certain. The optimizations have also confirmed its existence. The corresponding geometric parameters, the vibrational frequencies, the charge population, the adiabatic dissociation energies, and the vertical electron affinities obtained using several theoretical methods employing the 6-311+G* basis set are also collected in Tables 1−6, respectively. This species ($COSiCO^+$ ($^2A''$)) is energetically higher than the $Si(CO)_2^+$ ($^2B_1$) species but lower than the $Si(OC)_2^+$ ($^2B_1$) species. The calculated energy separation relative to $Si(CO)_2^+$ ($^2B_1$) is within 21.2−25.1 kcal/mol at DFT/6-311+G* levels with an exception of the BHLYP/6-311+G* value (16.7 kcal/mol). All these DFT values except the BHLYP one are close to the MP2 results at the same basis set level, but the BHLYP value is in good agreement with the MP3, MP4, and CCSD(T) results at the same basis set level with and without inner-shell electron correlation. However, using MP2(full)/6-311+G* geometries, the energy separation obtained by enlarging the basis set to aug-cc-pvtz is within 21.6−27.8 kcal/mol by single-point calculations at MP_n (n = 2, 3, 4) and CCSD(T) full electron correlation levels. They are inconsistent with DFT/6-311+G* and the two MP2/6-311+G* results. Although a common point of view is that DFT methods easily overestimate some energy quantities, the energy separation falling within 17−20 kcal/mol is reliable. Similarly, the energy separation of $COSiCO^+$ ($^2A''$) relative to $Si(OC)_2^+$ ($^2B_1$) may be predicted to be 13−18 kcal/mol. From these energy separations, it may be known that the $COSiCO^+$ ($^2A''$) species is energetically almost just between the $Si(CO)_2^+$ ($^2B_1$) and $Si(OC)_2^+$ ($^2B_1$) species. This has seemingly reflected such a phenomenon that there is almost no effect between the

two CO ligands in the $COSiCO^+$ ($^2A''$) complex. This character is closely related to the interaction properties between Si^+ and the two CO molecules.

For the Si−CO moiety, the optimized Si−C bond length is within 1.974−2.061 Å at several theoretical levels. The DFT results are slightly greater than the MP2 ones. Compared with those of the $Si(CO)_2^+$ ($^2B_1$) species, the Si−C bond length is longer by only 0.04−0.06 Å. For the C−O bond, the calculated values fall within 1.11−1.13 Å, and they are almost equivalent to those of the $Si(CO)_2^+$ ($^2B_1$) species. But the ∠SiCO angle in $COSiCO^+$ ($^2A''$) is greater by ∼8° than that in $Si(CO)_2^+$ ($^2B_1$). Only from these data can it be known that the property of the SiCO moiety of this species is almost similar to that of the $Si(CO)_2^+$ ($^2B_1$) species. For the SiOC moiety, the same phenomenon may be observed. The calculated Si−O bond lengths are 2.320 and 2.345 Å at the B3LYP/6-311+G* and BHLYP/6-311+G* levels, respectively, they are slightly longer than those (2.228 and 2.251 Å) obtained at the B3P86 and B3PW91 levels employing the same 6-311+G* basis set, but they are significantly shorter by 0.13−0.16 Å than the two MP2 results. No matter for the calculated bond lengths or for the deviations among these calculated values, they are almost equivalent to those in the $Si(OC)_2^+$ ($^2B_1$) species. The same is true for the C−O bond. But for the ∠SiOC angle, it is obviously smaller by ∼9° than that of the $Si(OC)_2^+$ ($^2B_1$) species. This angle change is just contrary with that of ∠SiCO of this molecule. In addition, the apex angle ∠CSiO is also very close to the apex angle ∠CSiC of $Si(CO)_2^+$ ($^2B_1$) and ∠OSiO of the $Si(OC)_2^+$ ($^2B_1$) species. These data have fully indicated that two CO molecules are basically freely coordinated to Si^+ ion by different terminals. The coupling interactions between them are small. In other words, it may also be said that there are almost the same coupling interactions between the two CO moieties in the $COSiCO^+$ ($^2A''$) species as those in the $Si(CO)_2^+$ ($^2B_1$) or in the $Si(OC)_2^+$ ($^2B_1$) species. These ∠SiCO and ∠SiOC angle changes, together with the Si−C and Si−O bond length changes, relative to those in the species without hybrid ligands have also implied another interesting aspect that although the interaction of Si^+ with the C-terminal of CO is stronger than that with the O-terminal of CO, the SiCO moiety becomes weaker relative to that in $Si(CO)_2^+$ ($^2B_1$) and tends to the structural character of the loose $Si^+\cdots CO$ species, while the SiOC moiety becomes stronger relative to that in $Si(OC)_2^+$ ($^2B_1$) and then tends to more bent due to the increased interaction between Si^+ and the in-side π^* orbital of CO. On the other hand, this outward bending also simultaneously reduces the repulsion interaction between two CO ligands and, thus, favors the linearization of the SiCO moiety.

Similarly, the vibrational frequencies also exhibit $COSiCO^+$ ($^2A''$) to be the intermediate between the $Si(CO)_2^+$ ($^2B_1$) and $Si(OC)_2^+$ ($^2B_1$) species. The ω_8 and ω_9 correspond to the symmetric and antisymmetric vibrational modes. The calculated frequencies are 2068−2281 cm^{-1} for ω_8 and 2174−2192 cm^{-1} for ω_9 at several methods except for the BHLYP method, which yields results slightly different from those of other methods. Comparison of these data with those of $Si(CO)_2^+$ ($^2B_1$) and $Si(OC)_2^+$ ($^2B_1$) species indicate that the ω_8 is almost equivalent to the $\omega_8(B_2)$ of $Si(OC)_2^+$ ($^2B_1$), and the ω_9 is much more close to the $\omega_9(A_1)$ of the $Si(CO)_2^+$ ($^2B_1$) species. Although the ω_8 and ω_9 are two coupling vibrations related to two moieties, they really reflect the vibrational properties of two CO moieties with different coordination modes from each other: one has the Si^+CO property of $Si(CO)_2^+$ ($^2B_1$), and the other behaves like the Si^+OC character of $Si(OC)_2^+$ ($^2B_1$). Another group of vibrational modes are ω_6 and ω_7, which correspond to the coupled Si−OC and Si−CO symmetric and antisymmetric stretching vibrations. The calculated results are also between the corresponding $\omega_6(B_2)$ and $\omega_7(A_1)$ values of the $Si(CO)_2^+$ ($^2B_1$) and $Si(OC)_2^+$ ($^2B_1$) species. The apex angle bending vibration also exhibits the same change relationship, viz., the bending frequency of ∠OSiC in the $COSiCO^+$ ($^2A''$) species is greater by 21−30 cm^{-1} than that of ∠OSiO in the $Si(OC)_2^+$ ($^2B_1$) species and is smaller by 20−35 cm^{-1} than that of ∠CSiC in the $Si(CO)_2^+$ ($^2B_1$) species. The same is true for the SiCO and SiOC bending vibrations. Overall, the above data analysis has also clearly verified the $COSiCO^+$ ($^2A''$) to be an intermediate between the $Si(CO)_2^+$ ($^2B_1$) and $Si(OC)_2^+$ ($^2B_1$) species no matter in structure or in property, agreeing well with the above analysis regarding stability and geometric parameters. The charge population in Table 2 has provided an evidence for this analysis from another aspect.

To further examine the bonding property and the relative stability of this species, the dissociation behavior has been tested according to three dissociation schemes:

$$COSiCO^+ (^2A'') \rightarrow SiCO^+ (^2\Pi) + CO \qquad (D_{e,1})$$

$$COSiCO^+ (^2A'') \rightarrow SiOC^+ (^2\Pi) + CO \qquad (D_{e,1'})$$

$$COSiCO^+ (^2A'') \rightarrow Si^+ (^2P) + 2CO \qquad (D_{e,2})$$

The calculated $D_{e,1}$ falls within 7.4−10.9 kcal/mol, while the calculated $D_{e,1'}$ value is 19−23 kcal/mol by ignoring some estimated values. These two groups of data have fully shown that the dissociation of the CO molecule with O-terminal coordination from the $COSiCO^+$ ($^2A''$) is easier than that of the CO molecule with C-terminal coordination from the $COSiCO^+$ ($^2A''$). The dissociation energy of CO with O-terminal coordination is almost equal to the first CO dissociation energy of $Si(OC)_2^+$ ($^2B_1$) (only slightly greater than that), while if the first dissociating CO is the CO with the C-terminal coordination, the dissociation energy ($D_{e,1'}$) is smaller by ∼5.0 kcal/mol than the first CO dissociation energy of the $Si(CO)_2^+$ ($^2B_1$) species. These small energy changes perhaps imply that there is a weak effect between the two CO coordinations to Si^+ by different terminals. This weak coupling interaction has resulted in the dissociation of CO with C-terminal coordination to be easier and that of CO with O-terminal coordination to be slightly more difficult, compared with those of the corresponding bicarbonyl and bi-isocarbonyl Si^+. This analysis is in good agreement with the geometry change and the frequency change. Of course, if we compare the total dissociation energies or the averaged dissociation energies of the three systems, we may also find similar regularity. But the total CO dissociation energy ($D_{e,2}$) of $COSiCO^+$ ($^2A''$) is not just equal to the average value of that ($D_{e,2}$) of $Si(CO)_2^+$ ($^2B_1$) and that ($D_{e,2}$) of the $Si(OC)_2^+$ ($^2B_1$) species. It is closer to the total dissociation energy of $Si(OC)_2^+$ ($^2B_1$), indicating that the contribution from the SiOC component increases and the contribution from the SiCO component decreases.

However, although there is the different effect from two CO ligands with different terminal coordinations, the vertical electron affinity exhibits well the average tendency. The EA_v of $COSiCO^+$ ($^2A''$) is almost equal to the average value of the $Si(CO)_2^+$ ($^2B_1$) EA_v and the $Si(OC)_2^+$ ($^2B_1$) EA_v. This phenomenon has fully demonstrated that for all three complexes the orbitals accepting electrons, viz., the lowest unoccupied molecular orbitals, are basically the pure Si atomic orbitals or

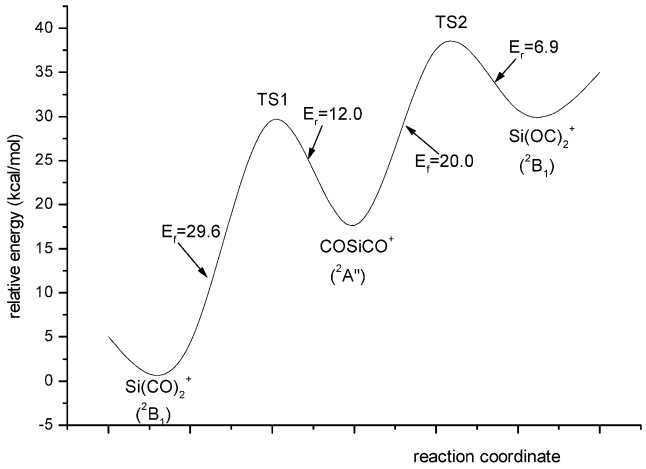

Figure 3. State−state correlations and isomerization mechanism among several isomers. E_f denotes the forward activation barrier, and E_r denotes the reverse one for the process from the left to the right. All energies are in kcal/mol and are obtained at the CCSD(T,full)/6-311+G*//MP2(fc)/6-311+G* level.

its hybrid orbitals, instead of the combined molecular orbital of Si atomic orbitals with CO molecular orbitals.

3.4. Isomerization Mechanism. To find the correlations among three isomers mentioned above, the transition state structure searches have been carried out using several theoretical methods employing the 6-311+G* basis set, and the corresponding state−state isomerization pathways have also been established using the intrinsic reaction coordinate (IRC) method and have also been confirmed by scanning the relaxed potential energy surface (PES) against ∠CSiO. The state−state correlations are described in Figure 3. From Figure 3 it can be known that the isomerization from $Si(CO)_2^+$ ($^2B_1$) to $Si(OC)_2^+$ ($^2B_1$) may experience a two-step mechanism including two transition states and one intermediate. This intermediate is just the $COSiCO^+$ ($^2A''$) species. For the two transition states, each one contains a three-membered ring moiety. No transition state is found for the direct correlation between the $Si(CO)_2^+$ ($^2B_1$) and $Si(OC)_2^+$ ($^2B_1$) species. No double ring intermediate or transition state has been found. At five theoretical levels, the optimized structural parameters, the charge population, the spin density, and the harmonic frequencies have been given in Tables 1−3. The state−state energy separations, ΔE, relative to the ground-state species $Si(CO)_2^+$ ($^2B_1$) are given in Table 4. From Table 4, the activation energies of these isomerizations may be extracted. For these isomers, although $Si(CO)_2^+$ ($^2B_1$) cannot directly correlate to $Si(OC)_2^+$ ($^2B_1$), they may isomerize into each other by undergoing two transition states and one intermediate.

As mentioned above, since these isomers are weakly bound complexes, the coordination interaction between the center Si^+ cation and the ligand CO is very weak, these molecules are structurally metastable or thermodynamically unstable, and thus are fragile. Furthermore, since these two transition states are energetically significantly higher than these stationary states, it may be further predicted that the transition state structures are much more unstable and the coupling interaction in both transition state complexes is much smaller. Obviously, the optimizations regarding these very weak interaction complexes have presented a serious challenge to theoretical chemists. The difficulties mainly concern behavior in three aspects: (1) the SCF convergence problem, (2) the potential energy surface is more flat, and (3) the transition state energy is close to the dissociated state energy. These difficulties must cause the location of the transition state to be more difficult. Therefore, from this viewpoint, it is also very interesting to explore the isomerization PES and to investigate the isomerization mechanism for these weakly bound complexes.

Actually, the TS1 may be obtained without some difficulties, while the TS2 cannot be easily located by directly using the methods mentioned above with the 6-311+G* basis set. But by changing the 6-311+G* basis set into the 6-31G* basis set, the TS2 can be located. So for the TS2, we first use four DFT methods and the frozen-core MP2 method with the 6-31G* basis set to optimize the TS2 transition state geometry and harmonic frequencies, and we then perform single-point energy calculations using the same methods with the 6-311+G* basis set at the 6-31G* geometry to further determine the various energy quantities. These results have been confirmed by comparing the TS1 situation using the same scheme, indicating that DFT/6-31G* and MP2(fc)/6-31G* may effectively yield comparable results for the geometrical parameters, harmonic frequencies, charge population, spin density, and so forth. So it can be concluded that the results obtained by this scheme for TS2 are reliable and can be safely used to discuss the reaction mechanism.

Before we analyze the isomerization mechanism among three stationary species, it is very necessary to first discuss the structures and properties of two transition states. For the TS1, it is also a planar structure with one three-membered ring. One side basically keeps the SiCO structure (slightly bent); the other side becomes a Δ-SiCO ring structure. For the SiCO part, the optimized Si−C bond length is within 1.989−2.069 Å at several theoretical levels; these results are slightly greater by 0.05−0.10 Å than those of the $Si(CO)_2^+$ ($^2B_1$) species and are almost equivalent to those of the $COSiCO^+$ ($^2A''$) species. Similarly, the C−O bond lengths are also almost equivalent to those of $Si(CO)_2^+$ ($^2B_1$) and $COSiCO^+$ ($^2A''$) species, but the ∠SiCO angle is slightly greater than those in $Si(CO)_2^+$ ($^2B_1$) and $COSiCO^+$ ($^2A''$) species, and it tends to be linear. For the Δ-SiCO ring part, it is obviously formed by bending the SiCO moiety inward. The calculated Si−C bond lengths are significantly longer by about 0.9−1.1 Å than those of $Si(CO)_2^+$ ($^2B_1$), viz., those before the SiCO is bent to be a triangle. The formed Si−O bond length is about 2.92−3.22 Å, also tending to that in the SiOC moiety of the $COSiCO^+$ ($^2A''$) species (longer by 0.6−0.8 Å). The largest change should be the ∠SiCO angle, which changes from ∼13° outward bending with respect to the Si−C axis to 96−105° inward bending. The total angle change is about 109−118°. In the triangle ring, the Si−C bond is basically equivalent to the Si−O bond. Obviously, the contact distance of this isomerized CO fragment to the center Si^+ is ∼3.0 Å, significantly longer than general chemical bonds containing Si atom, indicating that the interaction between the Si^+ center and the CO moiety is very weak. Obviously, from the structural analysis it can be shown that the TS1 should be correlated to the $Si(CO)_2^+$ ($^2B_1$) and $COSiCO^+$ ($^2A''$). Namely, if the Si−C bond of the triangle SiCO fragment is broken, it will change into $COSiCO^+$ ($^2A''$), while if the Si−O bond of the triangle SiCO fragment is broken, it will convert to $Si(CO)_2^+$ ($^2B_1$). The intrinsic reaction coordinate following and the relaxed PES scanning have also confirmed the correlation.

For the TS2, it possesses a bent SiOC fragment and a three-membered ring structure, but it is pyramidal instead of planar. Namely, the Si−O bond in the bent SiOC fragment is not coplanar with the triangle SiCO fragment. For the bent SiOC part, the calculated Si−O bond length is within 2.200−2.216 Å at four DFT levels; this is shorter by about 0.11 Å than the

MP2 value without the inner-shell electron correlation. These results are smaller by ~0.14 Å than that of $Si(OC)_2^+$ ($^2B_1$) at the same theoretical level. The corresponding C−O bond in the same fragment is 1.14−1.16 Å, being slightly longer than that in the $Si(OC)_2^+$ ($^2B_1$) species. The ∠SiOC angle is also very close to that in $Si(CO)_2^+$ ($^2B_1$). Thus, it can be said that the bent SiOC fragment in the TS2 structure still keeps the same character as that in $Si(OC)_2^+$ ($^2B_1$). For the triangle ring SiCO part, it is structurally similar to that in TS1, but it intersects with another SiOC plane. The calculated Si−C bond lengths for this triangle ring fall within 2.76−3.10 Å at five different theoretical levels, being very close to those of TS1. Its C−O bond lengths are within 1.123−1.154 Å, also being close to those in TS1. The same is true for the ∠SiCO angle. Since the C−O bond is still very strong, and cannot be easily broken, and the Si−O bond and Si−C bond may be classified as weak interactions, there are only two more easily breaking-bond modes for the three-membered ring: One is to break the Si−C bond, changing into the $Si(OC)_2^+$ ($^2B_1$) species. Another is to break the Si−O bond, converting to structure C, $COSiCO^+$ ($^2A''$). Thus, we can undoubtedly assign this TS2 structure to be a transition state correlating with $COSiCO^+$ ($^2A''$) and $Si(OC)_2^+$ ($^2B_1$).

The above analysis has assigned how the two transition states and three stationary states correlate to each other only from the geometrical viewpoint. Obviously, the charge population and the spin density distribution given in Table 2 also support these correlations. The positive charge over the Si^+ center is about 0.66−0.73 e for TS1; it is between those of $Si(CO)_2^+$ ($^2B_1$) and $COSiCO^+$ ($^2A''$) and is closer to that of the $COSiCO^+$ ($^2A''$) species. However, for TS2, the calculated positive charge over the Si^+ center falls within 0.77−0.82 e, being between that (0.79−0.85 e) of $Si(OC)_2^+$ ($^2B_1$) and that (0.70−0.76 e) of $COSiCO^+$ ($^2A''$), and it is closer to that in $Si(OC)_2^+$ ($^2B_1$). The same is true for the spin density distribution.

From Table 4, it can be known that these two transition states are energetically significantly higher than their correlated stationary states. For TS1, they are higher by 29.6 kcal/mol than the most stable species $Si(CO)_2^+$ ($^2B_1$) and also higher than the structure B, $COSiCO^+$ ($^2A''$), and almost equivalent to the stationary state $Si(OC)_2^+$ ($^2B_1$). This energy separation is also very close to the first CO dissociation energy, $D_{e,1}$(A), of $Si(CO)_2^+$ ($^2B_1$). The comparison has qualitatively reflected the instability of TS1. Checking the dissociation energy of TS1 may tell us that its dissociation energy is only a few kilocalories per mole, also indicating that it is a very weak interaction system. For TS2, its energy separation relative to the most stable species, $Si(CO)_2^+$ ($^2B_1$), is 36.7 kcal/mol at the CCSD(T,full)/6-311+G*//MP2(fc)/6-311+G* level. It is obviously higher in energy than the high-energy stationary $Si(OC)_2^+$ ($^2B_1$) species by about 7 kcal/mol. The energy separation of TS2 relative to $Si(OC)_2^+$ ($^2B_1$) is about 7 kcal/mol and very close to the first CO dissociation energy, $D_{e,1}$(C), of the $Si(OC)_2^+$ ($^2B_1$) species. Apparently, this energy separation is qualitatively close to the dissociation limit, implying that these transition states are really the loose ones. The corresponding isomerization process actually adopts the loosening−rotation mechanism. Namely, this mechanism includes two steps: (1) loosening the coupling interaction between Si^+CO and CO first and (2) then rotating the CO. This obviously is the isomerization character of the very weak interaction systems.

For $Si(CO)_2^+$ ($^2B_1$) species, optimizations have indicated that only one isomerization pathway may undergo, viz., isomerization into $COSiCO^+$ ($^2A''$) species by experiencing the TS1 transition state. The forward and backward activation energies are 28.7−33.1 and ~12.0 kcal/mol, respectively, indicating the backward isomerization is easier than the forward one. Going ahead, the COSiCO ($^2A''$) species may further isomerize into the $Si(OC)_2^+$ ($^2B_1$) one by surmounting TS2. The forward and backward activation energies are 20.0 and 6.9 kcal/mol at the CCSD(T,full)//MP2(fc) level with the 6-311+G* basis set, respectively. Obviously, it is also true that the isomerization from $Si(OC)_2^+$ ($^2B_1$) to the $COSiCO^+$ ($^2A''$) is easier than its inverse process. However, for the $Si(CO)_2^+$ ($^2B_1$) species, it also has only one isomerization pathway, viz., isomerization into the $COSiCO^+$ ($^2A''$) intermediate and further into the most stable species, $Si(CO)_2^+$ ($^2B_1$), by experiencing two transition states. This process is easier than the inverse one. Similarly, for the intermediate $COSiCO^+$ ($^2A''$) species, there are two possible isomerization pathways: one is to produce the $Si(CO)_2^+$ ($^2B_1$); the other is to produce the $Si(OC)_2^+$ ($^2B_1$). The activation energy barrier of the former is significantly higher than that of the latter. Together with the relative stability analysis, this observation has clearly indicated that when Si^+ is injected into the CO matrix, the main product should be $Si(CO)_2^+$ ($^2B_1$), and the other two species ($COSiCO^+$ ($^2A''$) and $Si(OC)_2^+$ ($^2B_1$)) with isocarbonyl coordination may also stably exist, but they are easily converted into the most stable isomer, $Si(CO)_2^+$ ($^2B_1$). In the other words, on the surface of the crystal Si materials or the noncrystal Si materials, perhaps there are many $Si^{\delta+}$ active centers. These active centers may easily absorb CO molecules to form $Si(CO)_2^+$, $COSiCO^+$, $Si(OC)_2^+$ or $Si_n(CO)_2^+$, $Si_n(CO)(OC)^+$, $Si_n(OC)_2^+$, and so forth. From the above analysis, although these complexes belong to the weak interaction complexes, the coupling interaction between the Si^+ or $Si^{\delta+}$ active centers and the CO molecules may also considerably change the structures and properties of the active centers or the materials' molecular surfaces related to the active centers. This kind of effect on the materials' structures and properties may change subject to the coupling mode between the Si^+ or $Si^{\delta+}$ active centers and CO molecules.

Obviously, the $Si(CO)_2^+ \rightarrow$ TS1 $\rightarrow COSiCO^+$ and $COSiCO^+ \rightarrow$ TS2 $\rightarrow Si(OC)_2^+$ isomerization processes are two endothermic ones, and their forward activation energies are large and, thus, are of the thermodynamic control, while their inverse processes are surely exothermic ones but the activation barriers are small and, so, are of the kinetic control. Therefore, we can select suitable conditions to control these isomerization processes and then further to improve the structures and properties of the materials' molecular surfaces.

4. Conclusion

On the basis of the important application of the crystal and noncrystal silicon materials, the interaction of Si^+ (a model active center) with the adsorbate (carbonyl, CO) has been explored in this paper. First, the structures, properties, and bonding character for the Si binary carbonyl and isocarbonyl monovalent cations, $Si(CO)_2^+$ ($^2B_1$), $(CO)Si(CO)^+$ ($^2A''$), and $Si(OC)_2^+$ ($^2B_1$), in their doublet states, have been investigated using four density functional theory (DFT) methods and the MP2 method with the 6-311+G* and aug-cc-pvtz basis sets. Results indicate that, for the binary carbonyl and isocarbonyl Si cations, there exist three stable isomers; all of them exhibit V-type structures in the doublet state, but no linear one has been found, being obviously different from that occurring in the transition metal carbonyl complexes. The most stable tautomer is $Si(CO)_2^+$ ($^2B_1$), the dicarbonyl Si cation, and can be assigned to the global energy minimum. The other two isomers are $(CO)Si(CO^+)$ ($^2A''$), the carbonyl and isocarbonyl Si cation, and

$Si(OC)_2^+$ ($^2B_1$), the di-isocarbonyl Si cation. They are 22.8 and 40.9 kcal/mol above $Si(CO)_2^+$ ($^2B_1$) at the CCSD(T)/aug-cc-pvtz level. The calculated results and bonding analysis have indicated that the binding strength of CO with Si^+ by the C-terminal is stronger than that by the O-terminal, but the C−O bond weakening caused by the O-terminal interaction with Si^+ is slightly greater than that by the C-terminal. The vertical electron affinities for three isomers also exhibit the same regularity as the CO binding energies. The vibrational frequencies and the charge populations also support the conclusion. These observations should be attributed to the difference between Si^+ and transition metal cations in the bonding orbital sets. These binary carbonyl or iso-carbonyl Si complex cations have essentially silene cation character and should be referred to as binary carbonyl silene. Due to the limitation of the bonding orbital sets and the special structural character, Si, other nonmetal atoms, and the nontransition metal atoms could not afford generally to form the polycarbonyl complexes with more than two CO ligands.

The transition state searches and the intrinsic reaction coordinate analysis have indicated that there are two single-ring transition states, in which TS1 correlates with $Si(CO)_2^+$ ($^2B_1$) and $(CO)Si(CO)^+$ ($^2A''$), and TS2 correlates with $COSiCO^+$ ($^2A''$) and $Si(OC)_2^+$ ($^2B_1$), respectively. The forward and reverse activation energies are 29.6 kcal/mol, 12.0 kcal/mol for TS1 and 20.0 kcal/mol, 6.9 kcal/mol for TS2, respectively. No direct correlation is found for $Si(CO)_2^+$ ($^2B_1$) and $Si(OC)_2^+$ ($^2B_1$). In general, the isomerization processes of this kind of weak system adopt the loosening−rotation two-step mechanism, viz. first the loosening of the coupling interaction between $SiCO^+$ and CO, and then the rotating of the ligand CO, indicating a different isomerization character from that occurring in the strong interaction systems.

Although the coupling interaction between Si^+ and CO is generally weak, it may change the property of the Si^+ active centers and the electronic structural character. It can be predicted that the weak coupling adsorption interaction of some small molecule ligands with the Si-active-centers-containing materials' macromolecules or the materials' surfaces may considerably affect the structural character and the surface properties of the materials' macromolecules. Therefore, the detailed studies about not only the interaction among large molecules but also that between large and small molecules need to be paid further attention. Perhaps investigations on the interaction and bonding among such small molecules may provide some valuable information.

In addition, it should be noted that it is very important to consider the electron correlation effect in the calculations regarding this type of complex. A series of recent investigations reveal that although high-level electron correlation methods such as CCSD(T), QCISD(T), MRCI, CASSCF-MP2, and so forth can give more accurate structures and properties for this type of weakly bound complexes, they generally require a more expensive computer source and more time. Fortunately, all these DFT methods such as B3LYP, B3P86, BHLYP, B3PW91, and so forth not only can avoid these difficulties but also yield comparable accuracy for the geometrical information and frequencies of the systems in the ground state with the MP2 method and even other high-level methods (such as CCSD(T)). However, for the energy calculations such as the state−state energy separations and dissociation energies and so forth, in general, B3LYP, B3P86, and B3PW91 methods slightly overestimate the relative energy quantities, while the BHLYP method can yield results agreeing well with the CCSD ones. Additionally, on the basis of the geometries optimized at the DFT or MP2 level, the single-point calculations at the CCSD(T) level or the other high-level methods can also give comparable results for the energy quantities to that at the pure CCSD(T) level. Therefore, for the investigations on this type of weakly bound complex, the applicable and effective scheme should be that one can use DFT and MP2 methods to optimize the geometrical information and frequencies, and then use the single-point calculations with CCSD(T)//DFT or CCSD(T)//MP2 and so forth methods to obtain the accurate energy quantities.

Acknowledgment. This work is supported by the National Natural Science Foundation of China (20273040, 29973022) and Foundation for Key Teachers in University of State Ministry of Education of China.

References and Notes

(1) Staemmler, V. *Chem. Phys*. **1975**, *7*, 17.
(2) Ikuta, S. *Chem. Phys. Lett*. **1984**, *109*, 550.
(3) Del Bene, J. E. *J. Comput. Chem.* **1986**, *7*, 259.
(4) Walter, D.; Sievers, M. R.; Armentrout, P. B. *J. Mass. Spectrosc. Ion Processes* **1998**, *175*, 93.
(5) Alikani, M. E.; Bouteiller, Y. *J. Mol. Struct.* **1997**, *436*, 481.
(6) Alikani, M. E. *THEOCHEM* **1998**, *432*, 263.
(7) Pullumbi, P.; Bouteiller, Y.; Perchard, J. P. *J. Chem. Phys*. **1995**, *102*, 5719.
(8) Pullumbi, P.; Bouteiller, Y. *Chem. Phys. Lett.* **1995**, *234*, 107.
(9) Wesolowski, S. S.; Galbraith, J. M.; Schaefer, H. F., III. *J. Chem. Phys*. **1998**, *108*, 9398.
(10) Balaji, V.; Sunil, K. K.; Jordan, K. D. *Chem. Phys. Lett*. **1987**, *136*, 309.
(11) Wesolowiski, S. S.; Crawford, T. D.; Ferman, J. T.; Schaefer, H. F., III. *J. Chem. Phys*. **1996**, *104*, 3672.
(12) Zhang, L.; Dong, J.; Zhou, M. *Chem. Phys. Lett.* **2001**, *335*, 334.
(13) Zhang, L.; Dong, J.; Zhou, M. *J. Chem. Phys*. **2000**, *113*, 8700.
(14) Burkholder, T. R.; Andrews, L. *J. Phys. Chem*. **1992**, *96*, 10195.
(15) Riemer, W. H.; Zika, R. G. *Marine Chem*. **1998**, *62*, 89.
(16) Goldman, A.; Coffey, M. T.; Stephen, T. M.; Rinsland, C. P.; Mankin, W. G.; Hannigan, J. W. *J. Quant. Spectrosc. Radiat. Transfer* **2000**, *67*, 447.
(17) Jacox, M. E.; Milligan, D. E.; Moll, N. G.; Thompson, W. E. *J. Chem. Phys*. **1965**, *43*, 3734.
(18) Devillers, M. C. *C. R. Acad. Sci*. **1966**, *262c*, 1485. Brown, S. T.; Yamaguchi, Y.; Schaefer, H. F., III. *J. Phys. Chem. A* **2000**, *104*, 3603.
(19) Lembke, R. R.; Ferrante, R. F.; Weltner, W., Jr. *J. Am. Chem. Soc.* **1977**, *99*, 416.
(20) Stolvik, R. *J. Mol. Struct*. **1985**, *124*, 133.
(21) Petraco, N. D. K.; Brown, S. T.; Yamaguchi, Y.; Schaefer, H. F., III. *J. Phys. Chem. A* **2000**, *104*, 10165.
(22) DeKock, R. L.; Grev, R. S.; Schaefer, H. F., III. *J. Chem. Phys.* **1988**, *89*, 3016.
(23) Grev, R. S.; Schaefer, H. F., III. *J. Am. Chem. Soc.* **1989**, *111*, 5687.
(24) Petraco, N. D. K.; Brown, S. T.; Yamaguchi, Y.; Schaefer, H. F., III. *J. Chem. Phys.* **2000**, *112*, 3201.
(25) Archibong, E. F.; St-Amant, A. *Chem. Phys. Lett*. **1998**, *284*, 331.
(26) Bu, Y.; Song, X. *J. Chem. Phys*. **2000**, *113*, 4216.
(27) Bu, Y. *Chem. Phys. Lett.* **2000**, *322*, 503.
(28) Bu, Y.; Song, X.; Liu, C. *Chem. Phys. Lett.* **2000**, *319*, 725.
(29) Bu, Y.; Xiahou, C.; Song, X. *Chem. Phys*. **2001**, *271*, 229.
(30) Bu, Y. *Chem. Phys. Lett.* **2001**, *338*, 142.
(31) Bu, Y. *Chem. Phys.* **2001**, *273*, 103.
(32) Bu, Y.; Han, K. *J. Phys. Chem. A* **2002**, *106*, 11897.
(33) Bu, Y.; Cao, Z. *Theor. Chem. Acc*. **2002**, *108*, 293.
(34) Frisch, M. J.; Trucks, G. W.; Schlegel, H. B.; Gill, P. M. W.; Johnson, B. G.; Robb, M. A.; Cheeseman, J. R.; Keith, T.; Petersson, G. A.; Montgomery, J. A.; Raghavachari, K.; Al-Laham, M. A.; Zakrzewski, V. G.; Ortiz, J. V.; Foresman, J. B.; Peng, C. Y.; Ayala, P. Y.; Chen, W.; Wong, M. W.; Andres, J. L.; Replogle, E. S.; Gomperts, R.; Martin, R. L.; Fox, D. J.; Binkley, J. S.; Defrees, D. J.; Baker, J.; Stewart, J. P.; Head-Gordon, M.; Gonzalez, C.; Pople, J. A. *Gaussian 94*, Revision B.2; Gaussian, Inc.: Pittsburgh, PA, 1995.
(35) Becke, A. D. *J. Chem. Phys.* **1993**, *98*, 5648.
(36) Lee, C.; Yang, W.; Parr, R. G. *Phys. Rev. B* **1988**, *37*, 785.
(37) Stephens, P. J.; Devlin, F. J.; Ashvar, C. S.; Chabalowki, C. F.; Frish, M. J. *Faraday Discuss.* **1994**, *99*, 103.
(38) Perdew, J. P. *Phys. Rev. B* **1986**, *33*, 8822.
(39) Perdew, J. P. *Phys. Rev. B* **1986**, *34*, 7406.
(40) Perdew, J. P.; Wang, Y. *Phys. Rev. B* **1992**, *45*, 13244.